



Original Research Paper

## *Saccharomyces cerevisiae* secretion of recombinant bacteriophage endolysin LysKB317 inhibits *Limosilactobacillus fermentum* in corn mash fermentation

Shao-Yeh Lu<sup>1,\*</sup>, Maulik H. Patel<sup>2</sup>, Ronald E. Hector<sup>3</sup>, Michael J. Bowman<sup>3</sup>, Christopher D. Skory<sup>1</sup>

<sup>1</sup>U.S. Department of Agriculture, Agricultural Research Service, National Center for Agricultural Utilization Research, Renewable Product Technology Research Unit, Peoria, IL 61604, USA.

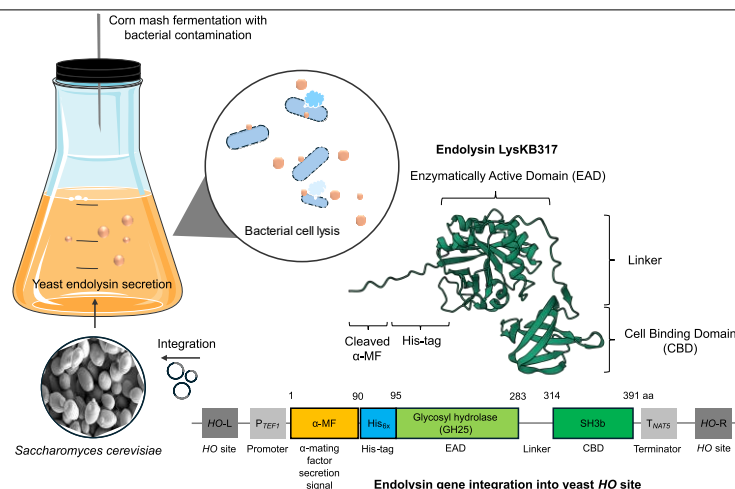
<sup>2</sup>Oak Ridge Institute for Science and Education (ORISE), Oak Ridge, TN, 37830, USA.

<sup>3</sup>The U.S. Department of Agriculture, Agricultural Research Service, National Center for Agricultural Utilization Research, Bioenergy Research Unit, Peoria, IL 61604, USA.

### HIGHLIGHTS

- > *HO*-locus integrated endolysin in yeast is genetically stable and expressed constitutively.
- > Yeast-secreted endolysin reduces bacterial contamination by more than 2-logs.
- > Secreted endolysin can reduce acetic and lactic acid levels by at least 60% in contaminated fermentation compared to untreated controls.
- > The system improves ethanol production by at least 16% in contaminated fermentations compared to untreated controls.
- > The secretion system provides sustainable and continuous bacterial contaminant control in corn mash fermentation and offers rapid industrial adaptability.

### GRAPHICAL ABSTRACT



### ARTICLE INFO

#### Article history:

Received 29 August 2024  
 Received in revised form 13 November 2024  
 Accepted 15 November 2024  
 Published 1 December 2024

#### Keywords:

Endolysin  
*Saccharomyces cerevisiae*  
 Yeast secretion  
 Fuel ethanol  
*Limosilactobacillus fermentum*  
 Antimicrobial

### ABSTRACT

This study investigated the secretion of endolysin LysKB317 integrated into the *HO* locus of *Saccharomyces cerevisiae* strain NRRL Y-2034 to enable the yeast to simultaneously perform ethanol fermentation and control bacterial contaminants frequently present in ethanol refineries. The cell wall hydrolase gene was expressed using *TEF1* and *NAT5* promoter and terminator sequences with  $\alpha$ -MF secretion signal and an N-terminus poly-histidine tag. LysKB317 was detectable by western blot analysis, which showed a molecular weight slightly larger than the 33 kDa native protein, presumably due to residual amino acids from the  $\alpha$ -MF secretion signal peptide or *S. cerevisiae* glycosylation. Secreted LysKB317 was confirmed to be active using turbidity reduction and cell viability assay. Contaminated corn mash fermentations with yeast secreting LysKB317 demonstrated a significant reduction in bacterial contamination by at least 2-log compared to the contamination controls without LysKB317 expression. Moreover, LysKB317 expression led to a 73% decrease in acetic acid concentration and a 67% decrease in lactic acid levels. Contaminated fermentations with yeast expressing LysKB317 also exhibited a 16% improvement in ethanol production over the contamination controls without LysKB317, with no significant difference observed when compared to yeast-only controls during a 72-h corn mash fermentation. These findings suggest that a yeast endolysin secretion platform holds promise for mitigating bacterial contamination in biorefineries and potentially reducing reliance on antibiotics usage.

©2024 Alpha Creation Enterprise CC BY 4.0

\* Corresponding author at:  
 E-mail address: [Shao.lu@usda.gov](mailto:Shao.lu@usda.gov)

## Contents

1. Introduction .....	2244
2. Materials and Methods .....	2246
2.1. Bacterial and yeast strains and growth conditions .....	2246
2.2. Constructs and plasmids .....	2246
2.3. Expression and purification of endolysin LysKB317 .....	2247
2.4. Western blot analysis .....	2247
2.5. Bacterial cell viability assay .....	2247
2.6. Turbidity assay .....	2247
2.7. Small-scale corn mash fermentation .....	2248
2.8. HPLC fermentation end products analysis .....	2248
2.9. Endolysin LysKB317 pH reversibility .....	2248
2.10. LC-MS/MS sample preparation .....	2248
2.11. LC-MS/MS analysis .....	2248
2.12. LC-MS/MS data analysis .....	2248
2.13. Statistical analysis .....	2248
3. Results and Discussion .....	2249
3.1. Endolysin expression confirmed through western blot .....	2249
3.2. Analysis of yeast-expressed LysKB317 .....	2249
3.3. Overnight yeast spent YPD media demonstrated lysis activity against <i>L. fermentum</i> .....	2250
3.4. Yeast-secreted endolysin LysKB317 for active mitigation of bacterial infection .....	2250
3.5. Expression of endolysin negates the negative effect of bacterial contamination during corn mash fermentation .....	2251
3.6. Impact of extracellular pH on the stability and functionality of secreted recombinant LysKB317 .....	2251
4. Conclusions .....	2253
Acknowledgments .....	2253
References .....	2253

### Abbreviations

2-ME	2-mercaptoethanol
ANOVA	Analysis of variance
BSA	Bovine serum albumin
CBD	Cell binding domain
CFU	Colony forming unit
CV	Column volume
EAD	Enzymatically active domain
FPLC	Fast protein liquid chromatography
HPLC	High-pressure liquid chromatography
IMAC	Immobilized metal affinity chromatography
IPTG	Isopropyl $\beta$ -D-1-thiogalactopyranoside
LAB	Lactic acid bacteria
LC-MS/MS	Liquid chromatography with tandem mass spectrometry
LiAc	Lithium acetate
MRS	De Man, Rogosa and Sharp
OD	Optical density
PEG	Polyethylene glycol
PVDF	Polyvinylidene difluoride
RPM	Revolution per minute
SD	Standard deviation
SDS-PAGE	Sodium dodecyl sulfate-polyacrylamide gel electrophoresis
TSA	Tryptic soy agar
TSB	Tryptic soy broth
YPD	Yeast extract peptone dextrose

The United States accounted for approximately 53% of global production in bioethanol at 15.6 billion gallons per year in 2023 (Kapetanakis et al., 2023; U.S. Energy Information Administration, 2023) and U.S. production is expected to grow as demand for renewable energy increases. The ethanol production process involves the conversion of sugar derived from biomass such as sugarcane, corn, and lignocellulosic materials into ethanol and carbon dioxide by fermentative microorganisms such as strains of *Saccharomyces cerevisiae* (Liu et al., 2016; Monteiro et al., 2018; Topaloglu et al., 2023). Although the fermentation process is efficient, it is prone to interference from contamination of microorganisms that negatively affect ethanol yield, resulting in costly production losses and extended downtime for cleaning and sterilization (Beckner et al., 2011). Lactic acid bacteria (LAB) are among the most common contaminants encountered in bioethanol refineries, specifically *Limosilactobacillus fermentum* strains (Skinner and Leathers, 2004; Skinner-Nemec et al., 2007; de Oliveira Lino et al., 2024). The presence of LAB competes for nutrient resources, alters fermentation kinetics, and leads to the accumulation of undesirable byproducts such as acetic acid and lactic acid (Rich et al., 2015). These organic acids inhibit yeast growth and metabolism, resulting in reduced ethanol productivity and stuck fermentations where the yeast becomes inactive before the fermentation process is complete (Narendranath et al., 2001; Graves et al., 2006; Walker and Basso, 2020).

Currently, the bioethanol industry in the United States and other regions of the world employ various chemical treatments, such as hop acids, chlorine dioxide, and antibiotics, to mitigate bacterial contamination (Rückle and Senn, 2006; Muthaiyan et al., 2011; Meneghin et al., 2008). However, countries within the European Union prohibit the use of antibiotics in bioethanol production and instead rely on energy-intensive heat sterilization (Hazards et al., 2021). In the U.S. and countries where permitted, antibiotics are used prophylactically to prevent unplanned fermentation facility shutdowns caused by acute fermentation contamination (Compart et al., 2013). This strategy, however, poses further risks, as prolonged exposure of bacteria to antibiotics can lead to the development of antibiotic-resistant bacteria within the fermentation system (Bischoff et al., 2007). This resistance diminishes antibiotic efficacy over time, necessitating higher doses, a combination of different drugs, or more expensive alternative treatments to achieve desirable outcomes.

In adherence to antibiotic stewardship and antibiotic-free production systems, alternative strategies to mitigate bacterial contamination are warranted. One promising approach is the use of alternative natural antimicrobial enzymes such as bacteriophage endolysins. Endolysins, a type of cell wall hydrolase, are employed by bacteriophages to lyse bacterial cell

## 1. Introduction

Bioethanol is an alternative to fossil fuels and offers reduction to greenhouse gas emissions and dependence on finite petroleum resources.

walls (peptidoglycan) at the end of the lytic replication cycle to release virion progeny (Bernhardt et al., 2002; Brady et al., 2021). While typically explored in clinical settings (Murray et al., 2021; Liu et al., 2023), our research and others have investigated their potential for controlling bacterial contamination in fermentation. To date, there have been no known reports on the development of resistance against the lysis activities of endolysin (Fischetti, 2005; Rahman et al., 2021), and experimentally, no resistance development has been observed, even after repeated treatments and passages of the bacterial strains with endolysin (Schmelcher et al., 2012). In the past decade, significant advancements have been made in endolysin-based control strategies for bioethanol fermentation (Fig. 1).

In 2013, we first demonstrated that the exogenous addition of recombinant bacteriophage endolysins was able to combat LAB contamination commonly found in corn mash bioethanol facilities (Roach et al., 2013). Since then, two other endolysins, LysKB317 (Lu et al., 2020) and LysMP (Patel et al., 2023), have been developed and shown to be effective enzyme-based biocontrols. While these enzymes offer targeted cell lysis and reduced bacterial resistance development, the exogenous application requires costly recombinant enzyme production and purification processes with potential batch-to-batch variability.

Bacteriophage, also known as phage, is a type of virus that infects bacteria (Podlacha et al., 2024). While these phages pose a threat to fermented food industries such as cheese, wine, and sauerkraut (Paillet and Dugat-Bony, 2021), they can be beneficial for the bioethanol refinery industry. Attempts to use phage-based strategies for direct application to ethanol fermentation have also been explored to target LAB contaminant (e.g., *L. fermentum*) known to cause stall fermentation or "stuck fermentation" (Silva and Sauvageau, 2014; Liu et al., 2015). Furthermore, Lin et al. (2015) applied encapsulation of bacteriophages with chitosan microspheres to combat bacterial contamination in yeast fermentations. These approaches are relatively simple and cost-effective but do suffer drawbacks such as narrow host range and potential bacterial resistance development (Schwarz et al., 2022a and b). Phage resistance can develop naturally through clustered regularly interspaced short palindromic repeats (CRISPR)-mediated mechanism, exposure to phage, exchange of plasmid, or cell receptor mutations (Charneco et al., 2023; Philippe et al., 2023).

Other innovative bacterial control strategies, such as probiotic-based

biocontrol (Rich et al., 2018), offer an environmentally friendly and sustainable alternative to antibiotics for managing bacterial control in fermentation. This approach utilizes probiotics already present in commercial fermentation tanks to control unwanted bacterial populations. However, its implementation can be challenging due to varying bacterial contaminant diversity from site-to-site.

Innovative biocontrol strategies, such as quorum-sensing-based approaches, were recently explored. The use of autoinducer-2 (AI-2) quorum-sensing inhibitors has shown promise in reducing bacterial growth and improving bioethanol yield in reducing bacterial competition against yeast for nutrients (Tian et al., 2024). Similarly, yeast-derived quorum-sensing molecules like 2-phenylethanol (2-PE) have been implicated in promoting ethanol fermentation (Tian et al., 2023). However, the challenges of bacterial contamination, species-specific requirements of AI-2 inhibitors, and economic factors associated with quorum sensing molecule production and application persist.

We propose that biocontrol of contaminants using *S. cerevisiae*-expressed endolysin is the most efficient and promising approach. This strategy leverages yeast's natural endolysin resistance and its ability to simultaneously produce the enzyme and ferment ethanol. Initial studies demonstrated the feasibility of intercellular endolysin production, but suboptimal enzyme performance and the requirement of galactose induction limited its practical application (Khatibi et al., 2014).

Kim et al. (2018) attempted to examine yeast secretion of endolysin; however, the result demonstrated limited improvement in sugarcane juice fermentation using *S. cerevisiae* as the expression host, which may be attributed to insufficient secretion levels and suboptimal endolysin activity. More recent research has shown promise in using *S. cerevisiae* cell surface display technology to simultaneously ferment ethanol and continuously treat lactic acid bacteria contaminants (Lu et al., 2023). While this approach offers potential, it requires continuous galactose induction and close-proximity between the bacterial contaminant and the surface-displayed endolysin for effective lysis.

In this study, we aim to address the limitations of previous endolysin delivery systems. We hypothesized that engineered yeast could constitutively express and secrete the endolysin LyKB317 to effectively mitigate bacterial contamination in bioethanol fermentation. To test this, we

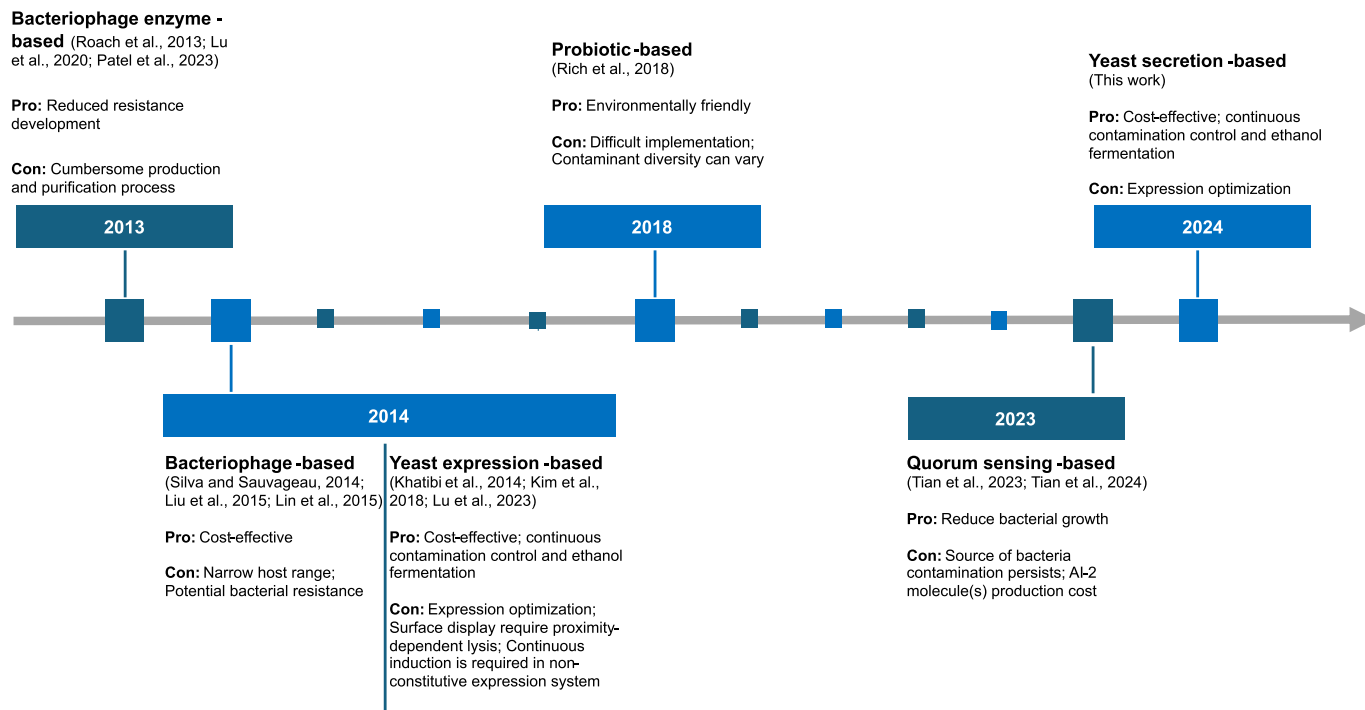


Fig. 1. A timeline schematic representation of the development of biocontrol strategies against bacterial contamination in bioethanol fermentation over the past decade.

integrate a yeast codon-optimized endolysin gene, LysKB317, at the *HO* locus of a yeast strain (*S. cerevisiae* NRRL Y-2034) for constitutive expression and secretion. We compared the engineered yeast in mitigating bacterial contamination, reducing acetic and lactic acid levels, and fermenting corn mash to the wild-type yeast control without contamination. The findings of this study demonstrated the feasibility of continuous ethanol fermentation alongside effective bacterial contaminant treatment without the use of traditional antibiotics or energy-intensive sterilization processes employed by the ethanol industries through engineering *S. cerevisiae* to secrete endolysin. This approach offers a more sustainable, economically viable, and practical solution compared to our previous cell surface display technology, eliminating the need for continuous galactose induction and proximity-dependent lysis in our previous approach (Lu et al., 2023).

## 2. Materials and Methods

### 2.1. Bacterial and yeast strains and growth conditions

All bacterial and yeast strains are listed in Table 1. Unless otherwise stated, all *Escherichia coli* strains were grown in tryptic soy broth (TSB; BD Biosciences) at 37°C and 200 rpm agitation. Antibiotics were added to TSB broth where appropriate at the following concentration: 100 µg/mL carbenicillin (Car; Sigma-Aldrich), 32 µg/mL chloramphenicol (Cm; Sigma-Aldrich) or kanamycin (Kan; Sigma-Aldrich) at 50 µg/mL. *L. fermentum* was grown using De Man, Rogosa, and Sharp broth (MRS; BD Biosciences) at 37°C without agitation. *S. cerevisiae* strains were grown in yeast extract peptone dextrose (YPD; BD Biosciences) at 30°C and 200 rpm agitation. Geneticin (G418; ThermoFisher Scientific) at 200 µg/mL was added to YPD broth for yeast strain selection when appropriate.

### 2.2. Constructs and plasmids

All plasmid and vector constructs are listed in Table 2. A *S. cerevisiae* codon-optimized LysKB317 gene, incorporating an alpha mating factor ( $\alpha$ -MF), N-terminal poly-His tag, and flanked by *TEF1* promoter and *NAT5* terminator, was synthesized commercially (GeneScript) in a pUC57-Kan

**Table 2.**  
Plasmid used in this study.

Plasmid <sup>a,b</sup>	Relevant Genotype	Reference
pUC57-Kan::P <sub>TEF1</sub> - $\alpha$ MF-LysKB317-T <sub>NAT5</sub>	Cloning vector containing <i>TEF1</i> promoter, alpha-mating factor, N-terminus 6×His-tag LysKB317, <i>NAT5</i> terminator	GenScript
pHO-poly- <sup>b</sup> KanMX4-HO	<i>HO</i> locus integration yeast vector	Voth et al. (2001)
pHO-poly-KanMX4-HO + P <sub>TEF1</sub> - $\alpha$ MF-LysKB317-T <sub>NAT5</sub>	<i>HO</i> locus integration yeast vector, contain <i>TEF1</i> promoter, $\alpha$ -MF, N-terminus 6×His-tag LysKB317, <i>NAT5</i> terminator	This Study

<sup>a</sup> Kan<sup>R</sup>, kanamycin-resistant.

<sup>b</sup> KanMX4, confers G418 resistance.

plasmid. The construct was transformed into chemically competent Top10 *E. coli* (Invitrogen) and selected on TSA (tryptic soy agar; BD Biosciences) plates containing 50 µg/mL Kan at 37°C. Gibson assembly (New England Biolabs) with primers (Table 3) was used to amplify insert from pUC57-Kan::P<sub>TEF1</sub>- $\alpha$ MF-N-terminus 6×His-tag LysKB317-T<sub>NAT5</sub> and to amplify pHO-poly-KanMX4-HO at the downstream 3' site of *HO*-Left locus and 5' upstream of *KanMX* selection marker.

The constructed vector, pHO-poly-KanMX4-HO + P<sub>TEF1</sub>- $\alpha$ MF-LysKB317-T<sub>NAT5</sub> (Table 2), was verified by Sanger sequencing. The vector was linearized with restriction enzyme NotI-HF (New England Biolabs) at 37°C for 1 h and inactivated at 65°C for 20 min. The desired fragment was gel purified and cleaned using a QIAquick PCR & Gel Cleanup kit (Qiagen), and concentration was determined with a spectrophotometer DS-11+ (DeNovix).

The *S. cerevisiae* strain NRRL Y-2034 was transformed using the protocol described by Gietz and Schiestl (2007). Briefly, yeast was grown to an optical density (OD<sub>600</sub> nm) of 1.0 (approximately 6 × 10<sup>7</sup> cells/mL) at 30°C and 150 rpm overnight in YPD. Cells were washed twice with ultrapure water and resuspended in 2 mL ultrapure sterile water to approximately 1 × 10<sup>9</sup> cells/mL before aliquoting 100 µL into 2 mL tubes

**Table 1.**  
Bacterial and yeast strains used for this study.

Bacteria and Yeast	Relevant Genotype/Phenotype <sup>a, b, c, d, e</sup>	Reference/Source <sup>f</sup>
<i>Escherichia coli</i>		
Top 10	F <sup>-</sup> mcrA $\Delta$ (mrr-hsdRMS-mcrBC) $\phi$ 80lacZ $\Delta$ M15 $\Delta$ lacX74 recA1 araD139 $\Delta$ (ara-leu)7697 galU galK $\lambda$ -rpsL(Str <sup>R</sup> ) endA1 nupG	Invitrogen
Top 10/pUC57-Kan::P <sub>TEF1</sub> - $\alpha$ MF-LysKB317-T <sub>NAT5</sub>	<sup>b</sup> Kan <sup>R</sup> , Cloning vector containing $\alpha$ -MF, LysKB317 gene flanked with <i>TEF1</i> promoter (P <sub>TEF1</sub> ) and <i>NAT5</i> terminator (T <sub>NAT5</sub> )	This Study
Top 10/pHO-poly- <sup>c</sup> KanMX4-HO	Yeast integration with target sequence at <i>HO</i> locus	(Voth et al., 2001); Addgene plasmid # 51661
Top10/ pHO-poly-KanMX4-HO +P <sub>TEF1</sub> - $\alpha$ MF-LysKB317-T <sub>NAT5</sub>	pHO-poly-KanMX4-HO plasmid containing $\alpha$ -MF, LysKB317 gene flanked with <i>TEF1</i> promoter (P <sub>TEF1</sub> ) and <i>NAT5</i> terminator (T <sub>NAT5</sub> )	This Study
BL21(DE3)/pLysS/pET21a(+):LysKB317	<sup>d</sup> Car <sup>R</sup> bacterial strain containing LysKB317 gene	This Study
<i>Limosilactobacillus fermentum</i>		
0315-25	Biofuel contaminant wildtype <sup>e</sup>	Lu et al. (2020); Rich et al. (2015)
<i>Saccharomyces cerevisiae</i> <sup>g</sup>		
NRRL Y-2034 (Y-2034 WT)	Bioethanol producing strain wildtype	Patel et al. (2023); NRRL <sup>f</sup>
Y-2034 – KB	Bioethanol producing strain with empty backbone (pHO-poly-KanMX4-HO) integrated in <i>HO</i> [hoD::KanMX4]	This Study
Y-2034 + KB	Bioethanol producing strain expressing LysKB317. <i>TEF1</i> promoter (P <sub>TEF1</sub> ), $\alpha$ -MF, N-terminus 6×His-tag LysKB317, and <i>NAT5</i> terminator (T <sub>NAT5</sub> ) integrated into <i>HO</i> .	This Study

<sup>a</sup>Str<sup>R</sup>, streptomycin-resistant; <sup>b</sup>Kan<sup>R</sup>, kanamycin-resistant; <sup>c</sup>KanMX4 confers G418 resistance; <sup>d</sup>Car<sup>R</sup>, carbenicillin-resistant.

<sup>e</sup>Wildtype microbial strain isolated from a midwestern dry-grind fuel ethanol facility and selected from a previous screen (Rich et al., 2015).

<sup>f</sup>USDA-ARS Culture Collection (NRRL).

Please cite this article as: Lu S.Y., Patel M.H., Hector R.E., Bowman M.J., Skory C.D. *Saccharomyces cerevisiae* secretion of recombinant bacteriophage endolysin LysKB317 inhibits *Limosilactobacillus fermentum* in corn mash fermentation. Biofuel Research Journal 44 (2024) 2243-2255. DOI: 10.18331/BRJ2024.11.4.4.

**Table 3.**  
Primers used for this study.

Primer Name	Primer Sequence (5' - 3') <sup>a</sup>	Purpose	Reference
50_2023	TGGAATTTTATGGTCCCGAGGTCACCCGGCCAGCG	Vector <i>pHO-poly-KanMX4-HO</i> inverse PCR; <b>BsiWI</b> and <b>BstEII</b> restriction site	This Study
51_2023	AAGTATGCATTGTTAGAGCTCGTACGACGCCATTTAAGTCCAAGGC		
52_2023	ACTTAAATGGCGTCGTACGAGCTCTAAACAATGCATACCTTTGTACGTT	Fragment insert of <i>P<sub>TEF1</sub></i> + $\alpha$ -MF + N-terminus 6×His-tag LysKB317+ <i>T<sub>NAT5</sub></i>	This Study
53_2023	TCGTGGCCGGGTGACCTCGGGACCATAAAAATTCATTAGGTCAG		
62_2023	CACCATCACCATCACCACGCTTTG	Sequence primer; LysKB317	This Study
63_2023	TCACCTGAAAGTACCAAAGCTTACCAGTGT		

<sup>a</sup>**Bold** represents restriction digestion sites.

for transformation. A mixture consisting of 240  $\mu$ L 50% w/v polyethylene glycol (PEG) 3,350 (Sigma-Aldrich), 36  $\mu$ L 1.0 M lithium acetate (LiAc; Sigma-Aldrich), 50  $\mu$ L 2.0 mg/mL denatured salmon sperm DNA (Sigma-Aldrich) in tris-EDTA buffer (Sigma-Aldrich) and 1  $\mu$ g DNA fragment was prepared. Then, heat-shocking of the yeast was performed with the combined mixture for 40 min in a 42°C-water bath, followed by centrifugation of cells to remove the supernatant. Five milliliters of YPD media were added to cells for recovery at 30°C and 150 rpm for 3 h, and 50  $\mu$ L of cells were placed onto the G418 selection YPD plate at 30°C up to 3 d. Successfully transformed yeast were verified for vector fragment integration using the primers listed in [Table 3](#) (Hector et al., 2023). Yeast-secreted endolysin was determined as explained in [Section 2.3](#), and activity was tested as described in [Sections 2.5](#) and [2.7](#).

### 2.3. Expression and purification of endolysin LysKB317

The expression of LysKB317 in *E. coli* was performed by growing a single colony of *E. coli* BL21(DE3) pLysS/pET21a(+):N-terminus 6×His-tag LysKB317 in TSB supplemented with Car and Cm at 37°C and 200 rpm to OD<sub>600nm</sub> of 0.6. The culture was induced overnight with 0.25 mM isopropyl  $\beta$ -D-1-thiogalactopyranoside (IPTG; Sigma-Aldrich) at a reduced temperature of 30°C and 200 rpm. Cells were harvested by centrifugation at 8,000  $\times$ g for 20 min at 4°C and lysed using B-PER<sup>TM</sup> Complete extraction reagent (ThermoFisher) per manufacturer's protocol. The lysate was centrifuged at 10,000  $\times$ g at 4°C for 5 min with supernatant filtered through a polyethersulfone (PES) 0.22  $\mu$ m membrane syringe filter (Millipore).

Filtered soluble protein fraction containing LysKB317 was purified using an ÄKTA pure<sup>TM</sup> (Cytiva) fast protein liquid chromatography using a 1-mL nickel-nitrilotriacetic acid (Ni-NTA) TALON<sup>®</sup> Superflow<sup>TM</sup> (Cytiva) column. The column was equilibrated with a five-column volume (CV) of equilibration buffer (300 mM NaCl in 50 mM phosphate (Sigma-Aldrich), pH 7.8) before loading cell lysate at a flow rate of 1 min/mL rate. After washing the column with 10 CV equilibration buffer, the protein was eluted in a single step gradient using 50% elution buffer (equilibration buffer with 300 mM imidazole (Sigma-Aldrich) and 10% glycerol (Sigma-Aldrich)). The purified LysKB317 (calculated 33.8 kDa) was verified by sodium dodecyl sulfate polyacrylamide gel electrophoresis (SDS-PAGE) on a 4% – 15% (w/v) precast stain-free tris-glycine sodium dodecyl sulfate polyacrylamide gel (Bio-Rad) and visualized using a ChemiDoc XRS+ imager (Bio-Rad). Protein concentration was quantified using a Qubit Protein Assay Kit (ThermoFisher) and a Qubit 3 fluorometer (ThermoFisher).

A single colony of yeast, *S. cerevisiae* Y-2034/*ho* $\Delta$ ::*KanMX*::*P<sub>TEF1</sub>*- $\alpha$ -MF-N-terminus 6×His-tag LysKB317-*T<sub>NAT5</sub>* (Y-2034 + KB) and *S. cerevisiae* Y-2034/*ho* $\Delta$ ::*KanMX* (Y-2034 – KB, no LysKB317 gene integration) were inoculated in separate 5 mL YPD media containing G418 at 30°C and 200 rpm. Cells were washed three times with 1 mL sterile PBS buffer (ThermoFisher) at 800  $\times$ g for 2 min and inoculated into 1-L fresh YPD media at 30°C and 200 rpm overnight. The spent media were centrifuged at 8,000  $\times$ g for 25 min at 4°C and filtered with Stericup<sup>®</sup> 0.22  $\mu$ m PES membrane filter (Millipore). Filtered sterile spent YPD media were further concentrated with a 15 kDa PES filter using a 500 mL Stirred cell reservoir (Amicon) with nitrogen air at pressure per manufacture protocol. A final concentrated volume of 100 mL from 1-L spent media was further purified using an FPLC using the method described above. The purified

protein (calculated at 34.1 kDa) was further verified with SDS-PAGE and quantified using a Qubit protein assay kit.

### 2.4. Western blot analysis

An SDS-PAGE containing LysKB317 was transferred onto a 0.2  $\mu$ m pore size low-fluorescence polyvinylidene difluoride membrane (PVDF; Bio-Rad) via a Trans-Blot Turbo transfer system (Bio-Rad). The membrane was blotted with Blocker BSA in TBS (ThermoFisher) for 1 h at room temperature with gentle agitation. Primary mouse anti-histidine-tag antibody (ThermoFisher) was applied at a 1:1,000 ratio in TBS-T (Tris-buffered saline containing 0.1% Tween-20; Sigma-Aldrich) and incubated overnight at 4°C with gentle swirling. After three washes with TBS-T, the membrane was incubated with a secondary goat anti-mouse antibody conjugated with Alexa fluor<sup>®</sup> 488 (ThermoFisher) at a 1:5,000 ratio for 1 h at room temperature. Following three additional washes with TBS-T, the membrane was imaged with a ChemiDoc XRS+ system.

### 2.5. Bacterial cell viability assay

To examine the exolytic activity of endolysin against target bacteria (*L. fermentum*), a fluorometric assay employing Sytox Green nucleic acid dye (ThermoFisher) was conducted using a previously described method (Harhala et al., 2021). Briefly, 50  $\mu$ L of a 1:1,000 dilution of Sytox Green dye in citric acid buffer (300 mM NaCl, 21 mM citric acid, 58 mM NaH<sub>2</sub>PO<sub>4</sub> and 30% (v/v) glycerol and pH buffer to pH 5.5; individual components from Sigma-Aldrich) were added to 100  $\mu$ L of *L. fermentum* cells at an OD<sub>600</sub> of 1 in a citric acid buffer.

Fifty microliters of 1  $\mu$ M endolysin (250 nM assay final) were added to a final reaction volume of 200  $\mu$ L per well. Positive and negative controls consisted of bacterial cells prepared in citric acid buffer without the addition of treatment. An addition of 50  $\mu$ L citric acid buffer was used in place of endolysin treatment. Bacterial cells were prepared by picking a single colony of *L. fermentum* 0315-25 and inoculating at 37°C in 5 mL MRS media as a pre-cultural followed by 1:100 ratio preculture passage into fresh 25 mL MRS and grown to OD<sub>600</sub> equivalent of 1 at 37°C. Cells were washed using citric acid buffer 3 times with centrifugation at 800  $\times$ g for 1 min. After washing, a portion of the cell was used as positive control by treating it with isopropanol (Sigma-Aldrich) for 20 min at room temperature with intermittent vortexing to agitate cells. The remaining cells were used as a negative control or for treatment. An iD5 SpectraMax (Molecular Devices) was used to measure relative fluorescence units (RFU) at excitation and emission wavelength 485 nm/535 nm for 1 h at room temperature using a black flat clear bottom 96-well plate (Corning). The mode of the read was set at median gain with a shake before the initial read for 15 sec and read every minute. All conditions were performed in 3 independent biological repeats ( $n = 3$ ).

### 2.6. Turbidity assay

The same 96-well microplates used for the cell viability assay mentioned above were also simultaneously analyzed to measure the optical density of the wells at OD<sub>600</sub> nm by a separate protocol using the SpectraMax iD5, and data exported using SoftMax Pro version 7.2 (Molecular Devices). Bacterial lytic activity (BLA) is defined in [Equation 1](#).

$$\text{BLA} = (\Delta\text{OD})/((\Delta\text{T})[\text{E}]) = \text{OD}/(\text{s})[\mu\text{M}] \quad \text{Eq.1}$$

where  $\Delta\text{OD}$  is the differences in optical density (OD) at 600 nm;  $\Delta\text{T}$  stands for the differences between time points in second (s); and  $[\text{E}]$  denotes the concentration of endolysin in micromolar ( $\mu\text{M}$ ).

### 2.7. Small-scale corn mash fermentation

To evaluate the efficacy of the yeast secretion system, small-scale corn mash fermentations were performed according to a previously described method (Lu et al., 2020; Patel et al., 2023) with some modifications. Briefly, corn mash obtained from a Midwest commercial dry-grind ethanol facility was dispensed in 16 mL aliquots into 25 mL Erlenmeyer flasks and incubated overnight for liquefaction at 40°C and 100 rpm with the addition of 10  $\mu\text{L}$  glucoamylase (Alcoholase II Liquid) and 240  $\mu\text{L}$  ammonium sulfate (0.12% w/v; Sigma-Aldrich). Yeast and bacteria strains (Table 1) were, respectively, grown overnight in YPD broth at 30°C and 200 rpm aeration and MRS at 37°C statically. Both overnight-grown yeast and bacteria strains were inoculated into corresponding fresh media to  $\text{OD}_{600} = 1$  for yeast (approximately  $6 \times 10^7$  CFU/mL) and  $\text{OD}_{600} = 4$  for bacteria (approximately  $1 \times 10^8$  CFU/mL). One hundred microliters of yeast (with and without LysKB317 integration) were added to corresponding flasks based on treatment or control conditions.

A two-hour acclimation period was given to yeast before 400  $\mu\text{L}$  of *L. fermentum* 0315-25 infection was added to the corn mash with 1 mL fresh MRS (to promote the growth of bacteria) and the addition of sterile water to a final volume of 20 mL. Rubber stoppers with a 20-gauge 0.9 mm  $\times$  40 mm Precision Glide needle (Becton Dickinson) were used to plug the flasks and to vent excess  $\text{CO}_2$  gas. Flasks were incubated at 30°C and 50 rpm for 72 h. At hours 0, 24, 48, and 72, samples (500  $\mu\text{L}$ ) were taken from each flask and serially diluted in ultra-pure water for bacterial counts on MRS agar supplemented with 100  $\mu\text{g}/\text{mL}$  cycloheximide (Sigma-Aldrich) using an Eddy Jet 2 spiral plater (IUL Instruments) set in the E mode 50 (50  $\mu\text{L}$  sample). Plated samples were incubated at 37°C overnight, and bacterial colonies were enumerated using a Flash & Go plate reader (IUL Instruments) with a minimum of detection limits predetermined at  $> 3$ -log (CFU/mL) per sample. Each condition was performed in 3 biological replicates ( $n = 3$ ). Selected fermentation metabolites were further quantified using HPLC, as described in Section 2.8.

### 2.8. HPLC fermentation end products analysis

A 300-mm Aminex HPX-87H column (Bio-Rad) at 0.5 mL/min using 5 mM  $\text{H}_2\text{SO}_4$  (Sigma-Aldrich) at 65 °C with a high-performance liquid chromatography system (HPLC; Shimadzu) coupled with a refractive index detector (RID) was used to detect residual glucose and fermentation metabolites (ethanol, acetic acid, and lactic acid).

### 2.9. Endolysin LysKB317 pH reversibility

To test LysKB317 exolytic activity when exposed to acid conditions in pH 3 and 4, fresh *E. coli* expressed recombinant LysKB317 purified by FPLC with concentration determination by Qubit protein assay kit, was aliquoted into three different pH (3, 4, and 5.5) citric acid buffer conditions (pH adjusted with HCl (Sigma-Aldrich) using a micro bulb pH electrode (Hanna Instruments); 300 mM NaCl, 30% (v/v) glycerol, 58 mM  $\text{NaH}_2\text{PO}_4$ , and 21 mM citric acid). Prior to conducting bacteria viability and turbidity assays, protein concentration was confirmed with Qubit protein assay and LysKB317 concentration was adjusted to 1  $\mu\text{M}$  to avoid inaccuracy of protein concentration due to insolubility of LysKB317 when exposed to pH 3 and 4 citric acid buffer. To assess endolysin's ability to re-gain its activity after acidic condition exposure (reversibility), protein concentration was re-evaluated with a Qubit protein assay kit and diluted to a concentration of 1  $\mu\text{M}$  in pH 5.5 citric acid buffer prior to running bacteria viability assay and turbidity assay using the methods mentioned in Sections 2.4 and 2.5.

### 2.10. LC-MS/MS sample preparation

IMAC-column purified fractions (from 2 L YPD media; 1.7 mL containing a total of  $\sim 150$   $\mu\text{g}$  protein) were concentrated (using a 10 kDa

nanosep spin column) to 200  $\mu\text{L}$ . The sample was dried in Speedvac (ThermoFisher), followed by redissolving in 100  $\mu\text{L}$  18 M $\Omega$  water. The sample was reduced in 5 mM dithiothreitol (DTT; Sigma-Aldrich) at 60°C for 45 min, allowed to cool to room temperature, followed by alkylation in 10 mM iodoacetamide at room temperature for 30 min. The sample was digested with 3  $\mu\text{g}$  trypsin (porcine pancreas, proteomics grade dimethylated, Sigma-Aldrich) in 100 mM ammonium bicarbonate (pH 7.95) incubated at 37°C for 18 h. The sample was dried, resuspended in 100  $\mu\text{L}$  18 M $\Omega$  water, and redried (2x), followed by resuspension in 100  $\mu\text{L}$  18 M $\Omega$  water + 0.1% formic acid (MS grade) and redried (2x). Finally, the sample was resuspended in 75  $\mu\text{L}$  18 M $\Omega$  water + 0.1% formic acid (MS grade) for unmodified peptide analysis.

To determine the presence of glycans on LysKB317, two separate methods were employed. For *O*-glycosylation determination a), treatment was essential, as described in Neubert et al. (2016); for *N*-glycosylation determination b), treatment was necessary, as in Poljak et al. (2018). After trypsin digestion, aliquots were dried, resuspended in 100  $\mu\text{L}$  18 M $\Omega$  water, and redried (3x), followed by resuspension in: a) 100 mM sodium acetate buffer (pH 4.6) + 2 mM zinc chloride and treated with  $\alpha$ -1,2,3,6 mannosidase (from Jack bean, New England Biolabs) at 37 °C for 18 h (according to the manufacturer's protocol) or b) 50 mM sodium acetate (pH 6.0) where *N*-glycans are trimmed down to a single HexNAc by the endoglycosidase H (Endo H) at 37 °C for 18 h according to the manufacturer's protocol (New England Biolabs). Samples were acidified to pH 2–3 with the addition of 18 M $\Omega$  water + 0.1% formic acid (MS grade) prior to MS analysis.

#### 2.11. LC-MS/MS analysis

Samples and controls were analyzed by LC-MS using a Vanquish HPLC equipped with an ODS-C18 column (3 mm  $\times$  150 mm, 3  $\mu\text{m}$  particle size, GL Sciences, Inc.), maintained at 50°C. Samples were maintained at 10°C in autosampler. Elution of analytes was accomplished at a flow rate of 0.550 mL/min by a programmed method as follows: 0–5 min maintained 5:95–95:5% 18 M $\Omega$  water + 0.1% formic acid (MS grade)(A): Optima grade methanol + 0.1% formic acid (MS grade)(B); followed by a linear gradient from 5:95 (A:B)–25:75% (A:B) over 30 min; followed by a linear gradient from 25:75 (A:B)–0:100% (A:B) over 3 min; followed by a holding at 0:100% (A:B) for 1 min; followed by a return to 5:95 (A:B) and re-equilibration for 8 min. The column effluent was monitored by UV at wavelengths 214 nm, 254 nm, and 280 nm prior to introduction into an Orbitrap ID-X- tribrid mass spectrometer (ThermoFisher) under Xcalibur 4.4 control. Mass spectral data from 200–2,000 Da  $m/z$  were collected in the orbitrap at 60,000 resolution. Tandem mass spectral data of ions between  $m/z$  400–2,000 exceeding  $2 \times 10^4$  counts were collected using collision-induced dissociation (CID, CE = 30) and higher-energy collision dissociation (HCD, CE = 25 and 30) in the Orbitrap analyzer at a mass resolution of 30,000.

#### 2.12. LC-MS/MS data analysis

Peptide identifications were determined using MaxQuant (Cox and Mann, 2008; Tyanova et al., 2016) software using a FASTA file based on the sequence of LysKB317, followed by comparison to the yeast proteome (reference from strain ATCC 204508 UP000002311 downloaded from UniProt.org at <https://www.uniprot.org/proteomes/UP000002311>) with LysKB317 inserted into the FASTA file and as well as common mass spectrometry protein contaminants. The precursor mass tolerance was set to 5 parts per million (ppm) and fragment ion mass tolerance to 2 ppm. Carbamidomethylation on cysteine (Cys) was used as a fixed modification, oxidation of methionine (Met), HexNAc of asparagine (Asn) (+ 203.079 Da) and hexosylation of serine (Ser) and threonine (Thr) (+ 162.052 Da) were used as variable modifications. A maximum of four variable modifications were allowed per peptide. A maximum of two missed trypsin cleavage sites were tolerated.

#### 2.13. Statistical analysis

Experimental results were analyzed using a two-way analysis of variance (ANOVA) with Tukey post-hoc test to determine statistical significance

where appropriate at  $**p < 0.005$ ,  $***p < 0.0001$ ,  $****p < 0.00001$  (GraphPad Prism version 10.2 and Microsoft Excel version 2401).

### 3. Results and Discussion

#### 3.1. Endolysin expression confirmed through western blot

The endolysin LysKB317 (GenBank accession number: AIY32273.1) gene encodes a 33.0 kDa enzyme that consists of a glycosyl hydrolase (GH25-like) domain and a single SH3b-like cell binding domain linked by a 31 amino acid linker (Fig. 2a; Lu et al., 2020). Protein structure prediction using RoseTTAFold (Fig. 2b; Baek et al., 2021) suggests that the addition of an N-terminal His<sub>6x</sub>-tag does not hinder the lytic activity of the GH25-like domain, making the full-length endolysin to 33.8 kDa.

Our previous research demonstrated the efficacy of exogenously adding purified recombinant endolysin to treat LAB contamination in corn mash fermentation at a laboratory scale (Lu et al., 2020). However, the shortcomings associated with the production cost of the enzyme pose a significant economic barrier for industrial-scale application. To address this limitation, we subsequently explored the yeast-surface display platform as a cost-effective delivery system for endolysin (Lu et al., 2023). While this approach would presumably lower the production cost associated with LysKB317, it relies on proximity-dependent cell-to-cell contact for effective bacterial lysis.

To improve industrial scalability and address the production cost and enzyme delivery challenges, we integrated LysKB317 into a bioethanol-producing *S. cerevisiae* strain (NRRL Y-2034). This engineered yeast strain enables simultaneous ethanol fermentation and endolysin secretion to control LAB contaminants, eliminating the need for proximity-dependent cell-to-cell contact.

We constructed an endolysin LysKB317 integration vector by using the *HO* locus integration plasmid (Fig. 2c). Variation of promoter combinations such as  $P_{ENO1}/T_{ENO1}$  with  $\alpha$ -MF and *Trichoderma reesei* xylanase 2, gene secretion signals (XYNSEC; Rossouw et al., 2023), and  $P_{CYC1}/T_{CYC1}$  (Mumberg et al., 1995), were assessed (results not shown). Only  $P_{TEF1}/T_{NAT5}$  with  $\alpha$ -MF produced detectable LysKB317 from the spent YPD media when visualized by SDS-PAGE after FPLC purification (Fig. 3a; Yamanishi et al., 2013). This promoter/terminator pair was chosen to maximize the expression of the endolysin. The *TEF1* promoter is a well-characterized,

highly active constitutive promoter from *S. cerevisiae* (Mumberg et al., 1995; Da Silva and Srikrishnan, 2012), and the *NAT5* termination sequence has been shown to improve mRNA stability, resulting in increased gene expression (Curran et al., 2013; Hector et al., 2019). Even though we could not visualize recombinant LysKB317 in spent media by SDS-PAGE due to other nonspecific protein bands present, in Western blot analysis, LysKB317 was clearly visualized (Fig. 3b). The molecular weight of the yeast-expressed endolysin was slightly larger than the expected 34.1 kDa (N-terminus EAEA-his<sub>6x</sub>-tag LysKB317) for both samples (concentrated spent media and FPLC elution fraction) when compared to the *E. coli* expressed LysKB317 (33.8 kDa N-terminus-his<sub>6x</sub>-tag LysKB317, Fig. S1), presumably due to residual amino acids from KEX2 endopeptidase cleavage of  $\alpha$ -MF secretion signal peptide (Seeboth and Heim, 1991; Le Marquer et al., 2019) or *S. cerevisiae* glycosylation.

#### 3.2. Analysis of yeast-expressed LysKB317

Tryptic-digested, yeast-expressed LysKB317 LC-MS/MS analysis resulted in peptide sequence coverage of 45%, identifying 13 peptides, 9 of which contained at least one Ser or Thr (accounting for 18 occurrences of these residues in the protein). Due to the heterogeneity of potential glycosylation, polydispersity of potential sites of glycosylation (35 Ser and Thr residues), or the lack of glycosylation, no evidence of glycosylation was found in the tryptic peptides. *S. cerevisiae* can glycosylate secreted proteins at Asn (*N*-linked) or Ser/Thr (*O*-linked) residues. *N*-linked glycosylation requires a consensus sequence of Asn-X-Ser/Thr, where X can be any amino acid. *O*-linked glycosylation by *S. cerevisiae*, however, is limited to *O*-mannosylation (Hausler et al., 1992; Gemmill and Trimble, 1999; Neubert et al., 2016). A study of the *O*-mannose glycoproteome of *S. cerevisiae* showed that approximately 26% of secreted proteins were *O*-mannosylated, where, based on the identified sites of *O*-mannosylation, it was reported that unstructured regions and  $\beta$ -strands containing high density of the Thr/Ser residues (20-50%; 4 – 10 residues in close proximity) were the criteria for *O*-mannosylation (Neubert et al., 2016).

To identify whether either of these glycosylations might be present, the samples were treated with  $\alpha$ -mannosidase or endoglycosidase H (Endo H), enzymes that hydrolyze glycan leaving a single carbohydrate residue (e.g., *O*-Mannose ( $\alpha$ -mannosidase) or *N*-HexNAc (EndoH)), thus converging any glycan heterogeneity to a single signal. However, these treatments did not

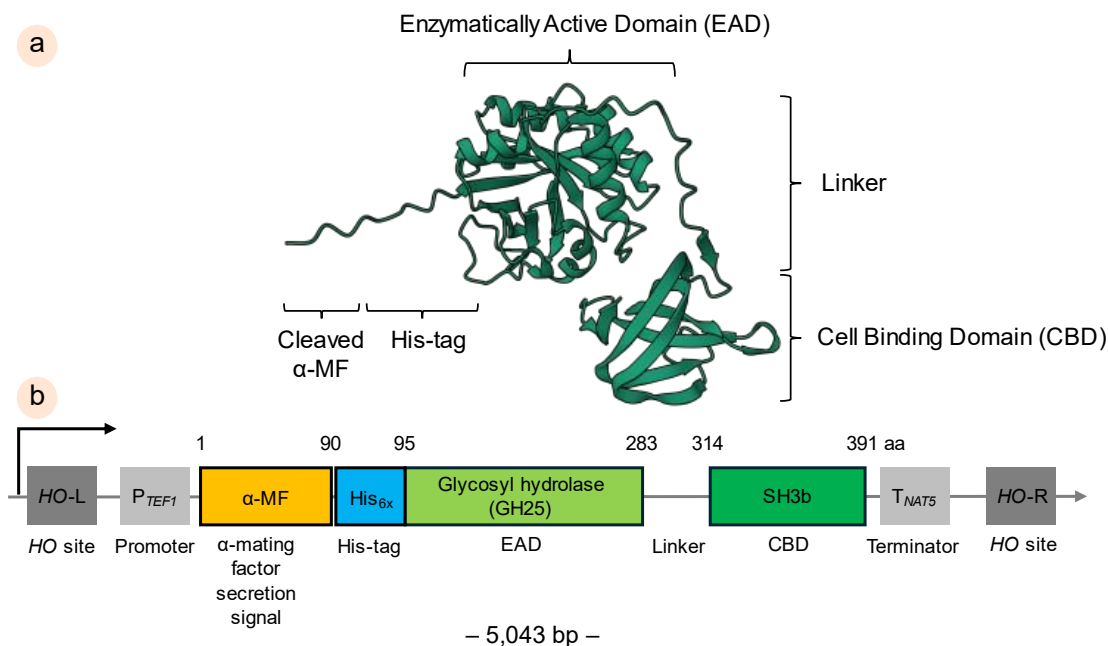


**Fig. 2.** Schematic representation of endolysin LysKB317 and its construct in a plasmid. (a) The recombinant endolysin LysKB317 depicting N-terminus 6-histidine epitope-tag with glycosyl hydrolase 25-like (GH25) enzymatically active domain (EAD) and SH3b-like cell wall binding domain (CBD). (b) The predicted three-dimensional model structure of LysKB317 by RoseTTAFold (Baek et al., 2021), and (c) Plasmid construct representation of LysKB317 gene using *pHO-poly-KanMX4-HO* (Voth et al., 2001).

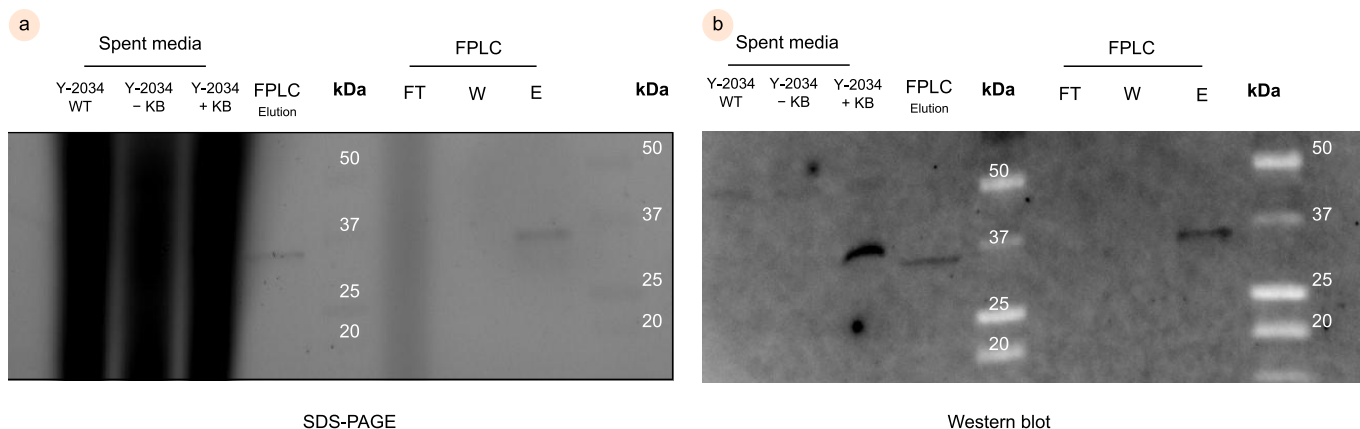


**Fig. 3.** *S. cerevisiae*-secreted LysKB317. The SDS-PAGE gel and Western blot of secreted and FPLC-purified endolysin LysKB317. (a) SDS-PAGE gel of spent media samples from yeast strains *S. cerevisiae* Y-2034 (Y-2034 WT), yeast with no endolysin integrated *pHO-poly-KanMX4-HO* (Y-2034 - KB), and *S. cerevisiae* Y-2034 with LysKB317 gene integrated (Y-2034 + KB). IMAC purification of N-terminus 6 × histidine-tagged LysKB317 (33.8 kDa) purification of spent media from Y-2034 + KB showing flow-through (FT), wash (W) and elution (FPLC<sub>Elution</sub>; E). Protein marker (kDa) Precision Plus Protein Standard (Bio-Rad), and (b) Western blot of the spent YPD media by yeast with no gene integrated control (Y-2034 - KB), and yeast with integrated LysKB317 (Y-2034 + KB) along with spent media purified using IMAC with flow-through (FT), wash (W) and elution (FPLC<sub>Elution</sub>; E) samples blotted onto polyvinylidene difluoride (PVDF) membrane and probed with mouse anti-6×His-tag and detected with goat anti-mouse antibody conjugated with Alexa488 (ThermoFisher). Yeast-spent media with secreted endolysin LysKB317 was detected at a molecular weight of approximately 36 kDa using the Precision Plus Protein reference standard.

reveal peptides with Ser/Thr or Asn residues modified with the respective single carbohydrate residue expected from the enzymatic treatment of the samples. This result is not unexpected, based on amino acid sequence criteria determined by Neubert et al. (2016). LysKB317 does not possess an amino acid sequence that is likely to be *O*-mannosylated, and the molecular weight difference is not great enough (< 1 kDa, 3-7 hexose residues based on SDS-PAGE molecular weight determination) to be caused by an *N*-linked glycan. However, due to the potential polydispersity (35 Ser and Thr residues) of *O*-linked mannose, glycosylation may occur at some sites. With a higher protein concentration and/or solid-phase extraction enrichment of glycosylated peptides, the uncharacterized 55% amino acid sequence coverage might reveal glycosylated peptides.

### 3.3. Overnight yeast spent YPD media demonstrated lysis activity against *L. fermentum*

Analysis of 1 μM LysKB317 purified from *E. coli* showed that maximum relative fluorescence units (RFU) of  $6 \times 10^6$  was achieved in 33 min. In the bacterial viability assay using Sytox Green, the bacterial lytic activity (BLA; Eq. 1) from 1 μM purified LysKB317 reached  $8.83 \times 10^{-5}$  ( $\Delta OD/(s)[\mu M]$ ) within the first 10 min, resulting in a 79 % reduction in optical density within 30 min (Figs. 4a and S2). In contrast, the concentration of yeast-secreted endolysin in spent media was significantly lower (approximately 0.34 μM), exhibiting an activity of  $2.70 \times 10^{-5}$  ( $\Delta OD/(s)[\mu M]$ ) during the first 30 min. This led to a 10% reduction in optical density at 30 min due to the lower endolysin concentration in the spent media at the time of testing (Figs. 4b and S3). Notably, the *S. cerevisiae* secretion system is continuous, and the concentration of endolysin LysKB317 would accumulate during the 72-h corn mash fermentation. The minimum lysis concentration of LysKB317 has been shown to be in the 3.9 nM range (Fig. S4).

### 3.4. Yeast-secreted endolysin LysKB317 for active mitigation of bacterial infection

As expected, wild-type yeast strain Y-2034 (Fig. 5: Purple bars; Y-2034 WT - Lf) without *L. fermentum* infection did not show a detectable bacterial number on MRS agar for the duration of 72 h. No significant difference (ns) in infection bacterial cell numbers was observed between yeast without LysKB317 integration (Fig. 5: Blue bars; Y-2034 - KB + Lf) vs. yeast with LysKB317 integration (Fig. 5: Red bars; Y-2034 + KB + Lf) at zero hour. The endolysin treatment group exhibited a 4% decrease in bacterial contamination from 0 to 48 h, while the untreated infection group showed a 21% increase. Significant differences in bacterial level were detected between treatment and no-treatment infection control groups at 24, 48, and

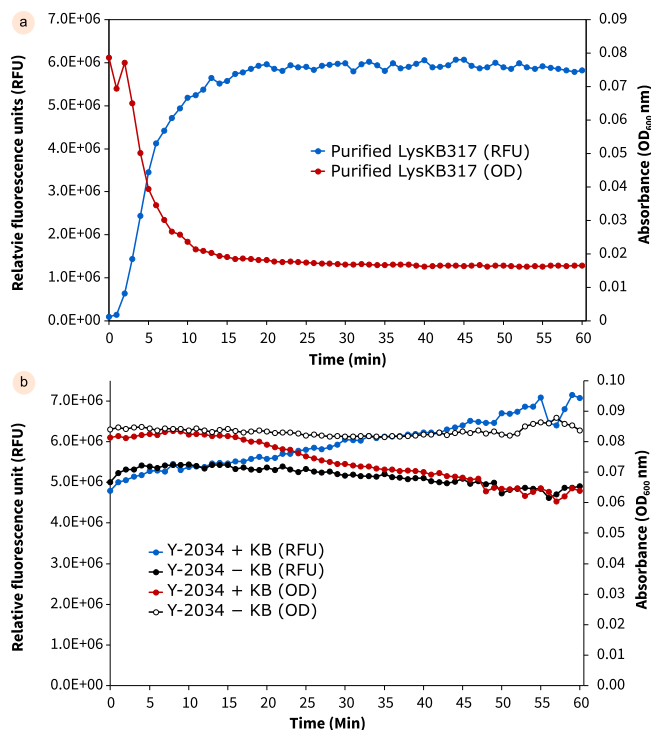


**Fig. 4.** Bacterial cell viability assay. (a) Cell viability was accessed using a Sytox Green nucleic acid stain (ThermoFisher) to examine the exolytic activity of *E. coli* expressed LysKB317 (1 μM at 250 nM final assay concentration) against *L. fermentum* 0315-25. Relative fluorescence units (RFU; Blue circle) indicate increased cell lysis overtime, as reflected by the increasing fluorescence signal. Turbidity reduction was measured by absorbance (optical density at 600 nm; Red circle), which showed a decrease in cellular density over time (60 min), consistent with endolysin-mediated cell lysis, and (b) Filtered overnight spent YPD media with (Blue for Sytox; Red for absorbance) and without (Black for Sytox; White for absorbance) secreted LysKB317 from yeast Y-2034 + KB and Y-2034 - KB culture tested for cellular lysis activity. Relative fluorescence units of Y-2034 + KB (Blue) showed increasing RFU signal with time compared to Y-2034 - KB (Black) remains flat. Turbidity assay measured by absorbance showed a decrease overtime in LysKB317 containing spent media (Red) and remains flat (White) for no LysKB317 spent media, indicating the effect of yeast-secreted endolysin.

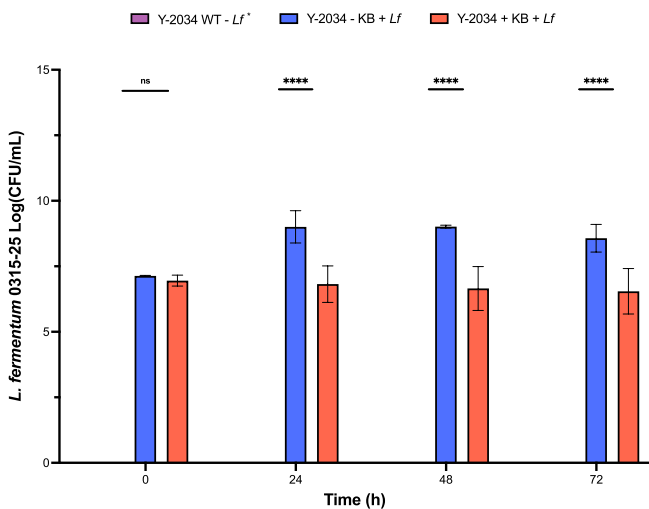


**Fig. 5.** Small-scale corn mash fermentation infection treatment with LysKB317 expressing *S. cerevisiae* for 72 h. Fermentation of corn mash was challenged with *L. fermentum* 0315-25 at  $10^6$  CFU/mL using yeast without LysKB317 gene (Infection control; Y-2034 - KB + Lf; Blue) and yeast with LysKB317 gene (Treatment; Y-2034 + KB + Lf; Red). The yeast-only control (Y-2034 WT) has no bacterial infection (Y-2034 WT - Lf; Purple). Asterisk (\*) indicates yeast control had no measurable *L. fermentum* presence. Bacterial counts were enumerated every 24 h and log-transformed to Log(CFU/mL). All measurements were performed with three independent biological replicates ( $n = 3$ ). \*\*\*\* $P < 0.00001$  based on two-way ANOVA, and error bars represent a 95% confidence interval (CI).

72 h ( $p < 0.00001$ ; Fig. 5). On average, a 2.2-log CFU/mL reduction in bacterial load was observed between the endolysin treatment and the no-treatment infection control from 24 to 72 h. This represents a 24% difference in bacterial load compared to the initial 2.5% difference at 0 h, and these differences in bacterial load successfully prevent yeast fermentation from stalling. Our yeast secretion system demonstrates the ability of the modified yeast to secrete LysKB317 and to continuously treat *L. fermentum* 0315-25 infection. This is a significant improvement to our previous efforts with yeast surface display of LysKB317 endolysin, which showed approximately 1-log CUF/mL reduction of bacterial contaminants in corn mash fermentation with continuous galactose induction for endolysin expression (Lu et al., 2023).

### 3.5. Expression of endolysin negates the negative effect of bacterial contamination during corn mash fermentation

To determine if the expression of secreted endolysin was beneficial to fermentation in the presence of bacterial contamination, small-scale corn mash fermentations were performed using the yeast strains expressing endolysin LysKB317 (strain Y-2034 + KB) in the presence of bacteria, *L. fermentum* (Figs. 6 and S4). Glucose utilization, ethanol production, and organic acid accumulation were measured every 24 h over a 72-h fermentation.

For comparison, a sample culture of wild-type Y-2034, without LysKB317 integration, was included without the addition of *L. fermentum* (Y-2034 WT). In cultures containing added bacteria and yeast cells not expressing endolysin, fermentation consistently slowed at 24, 48, and 72 h, with glucose utilization slowing by 11.8, 18.8, and 12.2%, respectively ( $p < 0.0001$ ) as bacteria-produced acids, hampering yeast fermentation and leading to "stuck fermentation" (Szopinska et al., 2016; Tse et al., 2021). Fermentation in these cultures was not completed in 72 h, and culture media had significant amounts of residual glucose at 14% (Y-2034, - KB, + Lf; Fig. 6a; Blue bars). Contrary to these results, corn mash cultures (Y-2034 WT) without added bacteria used all of the available glucose, and fermentation was complete in 48 h (Fig. 6a; Purple bars). Similar to cultures without added bacteria, cultures containing added bacteria and using yeast cells expressing endolysin were also able to consume all of the glucose and finished fermentation by 48 h (Y-2034, + KB, + Lf; Fig. 6a; Red bars), a 9.6-fold difference in glucose utilization ( $p < 0.0001$ ) compared to bacterial

contaminant control. Ethanol production results between strains mirrored results seen with glucose consumption (Fig. 6b). For cultures with added bacteria and not expressing endolysin, ethanol was still increasing at 72 h, and ethanol concentration (8.1% w/v ethanol) was 15.6% lower ( $p < 0.00001$ ) compared to no contamination control and LysKB317 treatment at 9.5% and 9.6% w/v, respectively. The ethanol production reached a maximum at 72 h for all groups. No difference in ethanol production was observed between control cultures without added bacteria and cultures with added bacteria that expressed endolysin by 48 h (Fig. 6b; Purple vs. Red bars). Ethanol production was 27% higher in the endolysin treatment group and no bacterial contamination group compared to contamination without treatment group at 48 h ( $p < 0.00001$ ). These results suggest that the integration of the expression cassette for endolysin LysKB317 is stable (Fig. S7) and did not negatively affect the strain's fermentation capability. Furthermore, it also shows that yeast cells expressing endolysin were able to negate the negative effects of bacterial contamination during corn mash fermentation, allowing complete glucose fermentation to ethanol by 48 h.

Analysis of organic acids (i.e., acetic and lactic acids) during corn mash fermentations showed that adding *L. fermentum* resulted in significant increases in both acetic and lactic acids by 7.8-fold and 18.8-fold, respectively ( $p < 0.00001$ ; Figs. 6c and 6d). This trend was observed starting at 24 h and continuing to the end of the fermentation. As expected, cultures without added bacteria did not show a significant increase in organic acids over the duration of fermentation. Cultures containing added bacteria and expressing endolysin showed an increase in both acetic and lactic acid levels, but the concentrations of these acids were reduced over time to a 2.2-fold and 0.2-fold increase, respectively ( $p < 0.00001$ ). Furthermore, endolysin-expressing yeast drastically reduced acetic acid and lactic acid concentrations by 5.6-fold and 12.4-fold, respectively, compared to cultures without endolysin expression for the duration of fermentation (Figs. 6c and 6d; Blue vs. Red bars). These results indicate that bio-mitigation of bacterial contamination by endolysin secreted by yeast in a small-scale corn mash fermentation can reduce the level of acetic and lactic acids and prevent stuck fermentation.

### 3.6. Impact of extracellular pH on the stability and functionality of secreted recombinant LysKB317

The pH of the extracellular environment is an important factor for the stability and functionality of the secreted recombinant protein (Salas-Navarrete et al., 2023). Yeast acidification of medium is a known phenomenon (Prins and Billerbeck, 2021), and acidophilic organisms such as *S. cerevisiae* work actively to maintain intracellular (pH 6.8; van Eunen et al., 2010) and extracellular pH between 4 to 6, but can be found at lower pHs (Imai and Ohno, 1995; Thomas et al., 2002; Narendranath and Power, 2005). Under anaerobic conditions, while conducting fermentation, the pH of the medium can decrease to 4.0 (Narendranath et al., 1997). Considering this, acidification of spent media or corn mash can negatively impact LysKB317 activity.

Our previous work established that LysKB317 has an optimal working pH of 6 and remains active between the range of pH 4 – pH 7.5 (Lu et al., 2020). However, under bacterial-contaminated fermentation conditions, the pH can drastically decrease from pH 5.5 to pH 3.5 at the end of fermentation and reduce and/or inactivate LysKB317 activity. For the duration of up to 72 h, the analysis of LysKB317 activity at pH 3 confirmed minimal activity compared to pH 4 and pH 5.5 (Figs. 7a, S5a-b, S6; and S8). Interestingly, when the pH was re-adjusted back to pH 5.5 from pH 4 or pH 3, LysKB317 activity was restored, indicating the reversibility of pH-induced inactivation of the enzyme (Figs. 7b, S5c-d, and S6). Thus, the inactivated endolysin under suboptimal pH conditions to an optimal pH condition is possible. Although yeast secretion of endolysin is effective in treating *L. fermentum* contaminant, the efficacy of endolysin LysKB317 for the duration of a 72-h fermentation can be lost after the first 24 h despite constitutive production and secretion of the endolysin. Further optimization of the endolysin is required to optimize the activity of LysKB317 under acidic conditions. A proposed application of the yeast secretion system involves its use in yeast culture propagation tanks, where the system can reduce bacterial contamination. As yeast propagates, the decrease in pH acidity can reduce endolysin's activity. However, pH re-adjustment prior to transferring yeast to the main tank can reactivate the LysKB317.

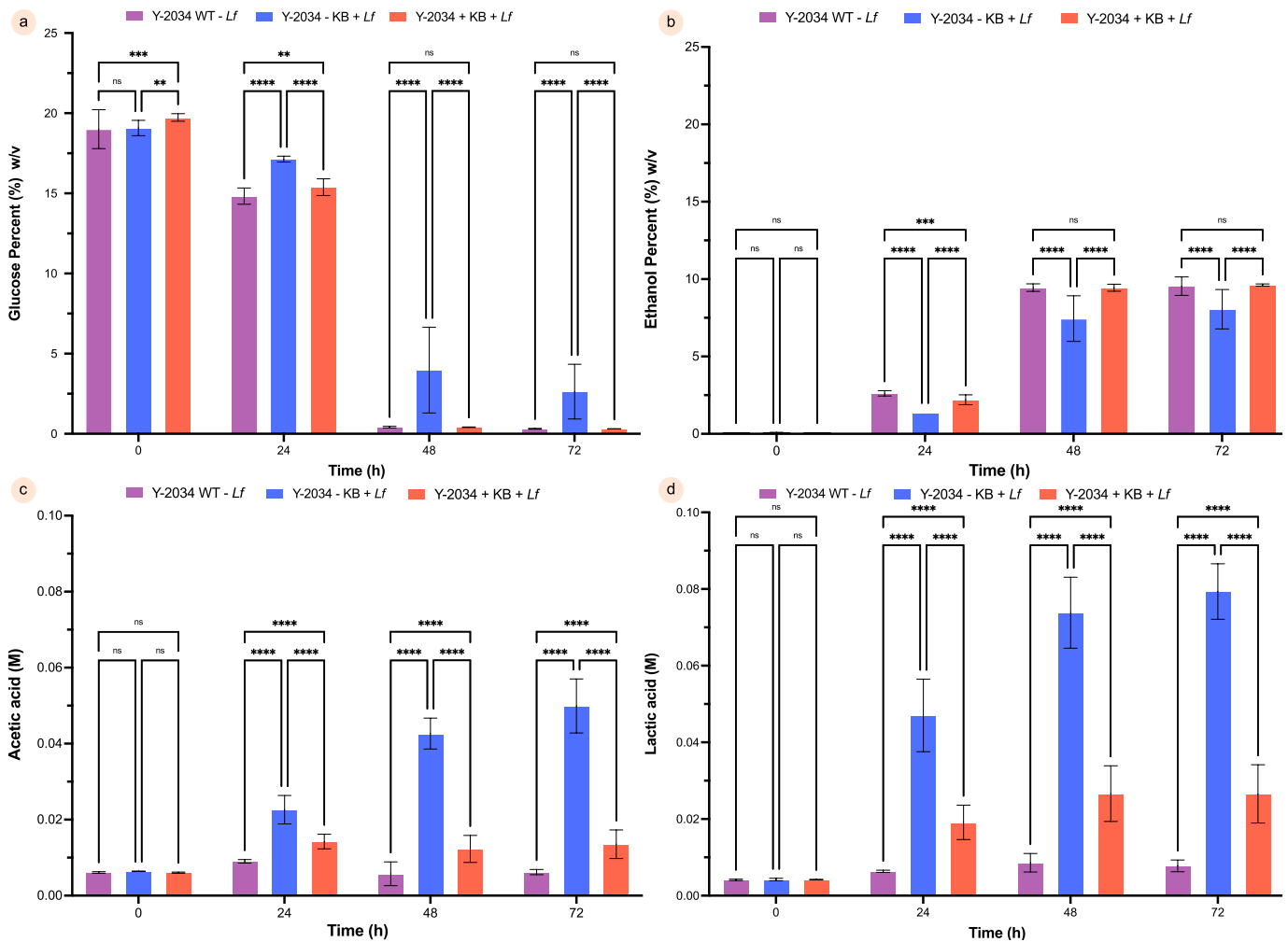


**Fig. 6.** HPLC analysis of corn mash glucose and fermentation metabolites. (a) Glucose consumption in percent (%) w/v; (b) Ethanol generated in percent (%) w/v; (c) molar (M) acetic acid; and (d) Molar (M) lactic acid. Yeast without LysKB317 gene integration (contamination control; Y-2034 - KB + Lf; Blue bars) and yeast with LysKB317 gene (Treatment; Y-2034 + KB + Lf; Red bars). The yeast-only control (Y-2034 WT; Purple bars) has no bacterial infection. All measurements were performed in three independent biological repeats ( $n = 3$ ) with mean  $\pm$  95% confidence intervals (CI). Statistically significant at \*\* $p < 0.001$ ; \*\*\* $p < 0.0001$ ; \*\*\*\* $p < 0.00001$  and no significant difference (ns) based on two-way ANOVA.

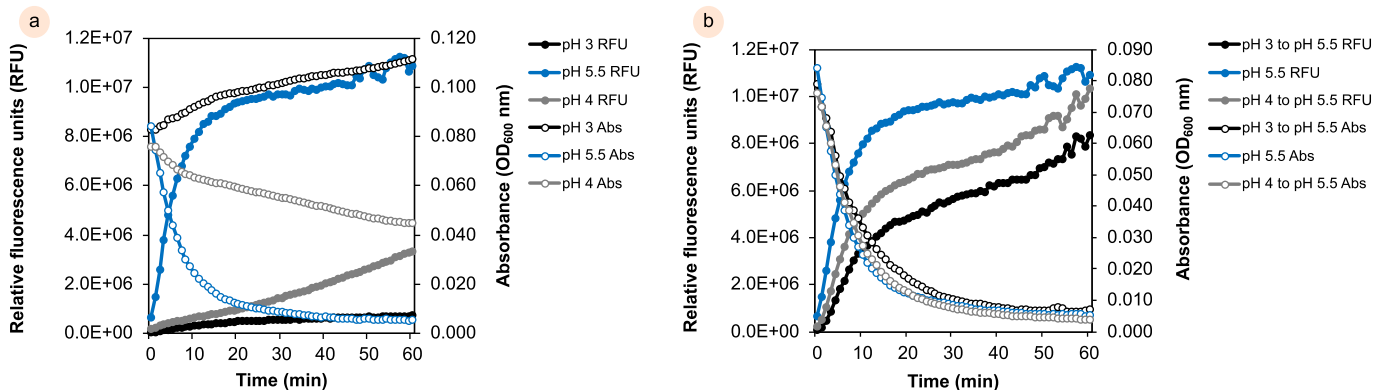


**Fig. 7.** Reversible activity of purified LysKB317 under acidic conditions. (a) Exolytic activity measuring relative fluorescence units (RFU) was assessed with purified LysKB317 (1  $\mu$ M) at pH 3 (Black), pH 4 (Grey), and pH 5.5 (Purple) using a Sytox Green nucleic acid stain (Left Y-axis). Turbidity assay of LysKB317 (1  $\mu$ M) under pH 3 (White), pH 4 (Grey open circle), and pH 5.5 (Blue) was measured by absorbance (OD<sub>600</sub> nm) by a microtiter plate reader (Right Y-axis). Results showed LysKB317 activity diminishes under pH 3 and pH 4 compared to pH 5.5, and (b) Endolysin LysKB317 activity restored upon re-adjustment of buffer pH to pH 5.5. Reversed acidic condition of purified LysKB317 from pH 3 to pH 5.5 (Black), pH 4 to pH 5.5 (Grey), and pH 5.5 (Purple) at 1  $\mu$ M. Relative fluorescence units (RFU; Left Y-axis) were measured. Turbidity assay measuring absorbance (OD<sub>600</sub> nm) of re-adjusted buffer pH, pH 3 to pH 5.5 (White), pH 4 to pH 5.5 (Grey open circle), and pH 5.5 (Blue) were measured (Right Y-axis). Results showed endolysin activity restored post buffer pH re-adjustment. All measurements were performed in three independent biological repeats ( $n = 3$ ) and statistically determined significance.

To advance yeast-endolysin secretion technology and facilitate its adaptation by the bioethanol industry, further development and optimization of the system are necessary at the pilot scale to assess its scalability at the industrial level. As part of the growing emphasis on antibiotic stewardship and sustainable production, this technology can reduce bacterial mitigation and bioethanol production costs. Techno-economic analysis (TEA) and life-cycle analysis (LCA) are crucial in providing valuable insights into the economic feasibility and environmental impact of the technology (Gheewala, 2023). Additionally, improving the expression level of LysKB317 and expanding its optimal acidic pH range can significantly enhance its usability. Alternatively, developing novel endolysin with improved efficacy could further optimize the system's performance. The technology's versatility allows for easy adaptation to various fermentation processes, including biomedical fermentation, food fermentation, and alternative biotechnology, such as precision fermentation, and enabling bacterial contamination control.

#### 4. Conclusions

In conclusion, fermentation using engineered yeast to secrete endolysin allows a proactive and continuous approach to address bacterial contamination in the bioethanol industry without relying on antibiotics. This strategy offers an effective and economical solution to mitigate the risk of stuck fermentation. By actively mitigating harmful bacteria and reducing the accumulation of bacterially produced organic acids such as acetic and lactic acids, the yeast developed in this study can enhance overall productivity more efficiently and sustainably without the use of antibiotics. The potential for direct adaptation in commercial ethanol production facilities underscores the significant industrial potential of this technology. To fully realize its potential, the bioethanol industry should consider exploring similar technology in commercial production facilities.

#### Acknowledgments

We thank Moses Y. Martinez and Kristina M. Glenzinski for their excellent technical assistance. This research was supported by the U.S. Department of Agriculture, Agricultural Research Service (USDA-ARS).

#### References

- Baek, M., DiMaio, F., Anishchenko, I., Dauparas, J., Ovchinnikov, S., Lee, G.R., Wang, J., Cong, Q., Kinch, L.N., Schaeffer, R.D., Millan, C., Park, H., Adams, C., Glassman, C.R., DeGiovanni, A., Pereira, J.H., Rodrigues, A.V., van Dijk, A.A., Ebrecht, A.C., Opperman, D.J., Sagmeister, T., Buhlheller, C., Pavkov-Keller, T., Rathinaswamy, M.K., Dalwadi, U., Yip, C.K., Burke, J.E., Garcia, K.C., Grishin, N.V., Adams, P.D., Read, R.J., Baker, D., 2021. Accurate prediction of protein structures and interactions using a three-track neural network. *Science*. 373(6557), 871-876.
- Beckner, M., Ivey, M.L., Phister, T.G., 2011. Microbial contamination of fuel ethanol fermentations. *Lett Appl Microbiol* 53(4), 387-394.
- Bernhardt, T.G., Wang, I.N., Struck, D.K., Young, R., 2002. Breaking free: "protein antibiotics" and phage lysis. *Res Microbiol* 153(8), 493-501.
- Bischoff, K.M., Skinner-Nemec, K.A., Leathers, T.D., 2007. Antimicrobial susceptibility of *Lactobacillus* species isolated from commercial ethanol plants. *J. Ind. Microbiol. Biotechnol.* 34(11), 739-744.
- Brady, A., Felipe-Ruiz, A., Gallego Del Sol, F., Marina, A., Quiles-Puchalt, N., Penades, J.R., 2021. Molecular Basis of Lysis-Lysogeny Decisions in Gram-Positive Phages. *Annu. Rev. Microbiol.* 75, 563-581.
- Charneco, G.O., de Waal, P.P., van Rijswijck, I.M.H., van Peij, N.N.M.E., van Sinderen, D., Mahony, J., 2023. Bacteriophages in the Dairy Industry: A Problem Solved? *Annu. Rev. Food Sci. Technol.* 14(1), 367-385.
- Compart, D.M., Carlson, A.M., Crawford, G.I., Fink, R.C., Diez-Gonzalez, F., Dicostanzo, A., Shurson, G.C., 2013. Presence and biological activity of antibiotics used in fuel ethanol and corn co-product production. *J. Anim. Sci.* 91(5), 2395-2404.
- Cox, J., Mann, M., 2008. MaxQuant enables high peptide identification rates, individualized p.p.b.-range mass accuracies and proteome-wide protein quantification. *Nat. Biotechnol.* 26(12), 1367-1372.
- Curran, K.A., Karim, A.S., Gupta, A., Alper, H.S., 2013. Use of expression-enhancing terminators in *Saccharomyces cerevisiae* to increase mRNA half-life and improve gene expression control for metabolic engineering applications. *Metab. Eng.* 19, 88-97.
- Da Silva, N.A., Srikrishnan, S., 2012. Introduction and expression of genes for metabolic engineering applications in *Saccharomyces cerevisiae*. *FEMS Yeast Res.* 12(2), 197-214.
- de Oliveira Lino, F.S., Garg, S., Li, S.S., Misiakou, M.A., Kang, K., Vale da Costa, B.L., Beyer-Pedersen, T.S., Giacon, T.G., Basso, T.O., Panagiotou, G., Sommer, M.O.A., 2024. Strain dynamics of contaminating bacteria modulate the yield of ethanol biorefineries. *Nat. Commun.* 15(1), 5323.
- Fischetti, V.A., 2005. Bacteriophage lytic enzymes: novel anti-infectives. *Trends Microbiol.* 13(10), 491-496.
- Gheewala, S.H., 2023. Life cycle assessment for sustainability assessment of biofuels and bioproducts. *Biofuel Res. J.* 10(1), 1810-1815.
- Gemmill, T.R., Trimble, R.B., 1999. Overview of N- and O-linked oligosaccharide structures found in various yeast species. *Biochimica et Biophysica Acta (BBA) - General Subjects.* 1426(2), 227-237.
- Gietz, R.D., Schiestl, R.H., 2007. Large-scale high-efficiency yeast transformation using the LiAc/SS carrier DNA/PEG method. *Nat Protoc.* 2(1), 38-41.
- Graves, T., Narendranath, N.V., Dawson, K., Power, R., 2006. Effect of pH and lactic or acetic acid on ethanol productivity by *Saccharomyces cerevisiae* in corn mash. *J. Ind. Microbiol. Biotechnol.* 33(6), 469-474.
- Harhala, M., Gembara, K., Miemikiewicz, P., Owczarek, B., Kazmierczak, Z., Majewska, J., Nelson, D.C., Dabrowska, K., 2021. DNA dye sytox green in detection of bacteriolytic activity: high speed, precision and sensitivity demonstrated with endolysins. *Front Microbiol.* 12, 752282.
- Hausler, A., Ballou, L., Ballou, C.E., Robbins, P.W., 1992. Yeast Glycoprotein-Biosynthesis - Mnt1 Encodes an Alpha-1,2-Mannosyltransferase Involved in O-Glycosylation. *Proc. Natl. Acad. Sci. USA.* 89(15), 6846-6850.
- Hazards, E.P.o.B., Koutsoumanis, K., Allende, A., Alvarez-Ordóñez, A., Bolton, D., Bover-Cid, S., Chemaly, M., Davies, R., De Cesare, A., Herman, L., Hilbert, F., Lindqvist, R., Nauta, M., Ru, G., Simmons, M., Skandamis, P., Suffredini, E., Andersson, D.I., Bampidis, V., Bengtsson-Palme, J., Bouchard, D., Ferran, A., Kouba, M., Lopez Puente, S., Lopez-Alonso, M., Nielsen, S.S., Pechova, A., Petkova, M., Girault, S., Broglia, A., Guerra, B., Innocenti, M.L., Liebana, E., Lopez-Galvez, G., Manini, P., Stella, P., Peixe, L., 2021. Maximum levels of cross-contamination for 24 antimicrobial active substances in non-target feed. Part 1: *Methodology, general data gaps and uncertainties.* *EFSA J.* 19(10), e06852.
- Hector, R.E., Mertens, J.A., Nichols, N.N., 2019. Development and characterization of vectors for tunable expression of both xylose-regulated and constitutive gene expression in *Saccharomyces* yeasts. *New Biotechnol.* 53, 16-23.
- Hector, R.E., Mertens, J.A., Nichols, N.N., 2023. Metabolic engineering of a stable haploid strain derived from lignocellulosic inhibitor tolerant *Saccharomyces cerevisiae* natural isolate YB-2625. *Biotechnol. Biofuels. Bioprod.* 16(1), 190.
- Imai, T., Ohno, T., 1995. The relationship between viability and intracellular pH in the yeast *Saccharomyces cerevisiae*. *Appl. Environ. Microbiol.* 61(10), 3604-3608.
- Kapetanakis, G.C., Sousa, L.S., Felten, C., Mues, L., Gabant, P., Van Nedervele, L., Georis, I., André, B., 2023. Deletion of *QDR* genes in a bioethanol-producing yeast strain reduces propagation of contaminating lactic acid bacteria. *Sci Rep.* 13(1), 4986.
- Khatibi, P.A., Roach, D.R., Donovan, D.M., Hughes, S.R., Bischoff, K.M., 2014. *Saccharomyces cerevisiae* expressing bacteriophage endolysins reduce *Lactobacillus* contamination during fermentation. *Biotechnol. Biofuels.* 7, 104.

- [25] Kim, J.S., Daum, M.A., Jin, Y.S., Miller, M.J., 2018. Yeast Derived LysA2 Can Control Bacterial Contamination in Ethanol Fermentation. *Viruses*. 10(6), 281.
- [26] Le Marquer, M., San Clemente, H., Roux, C., Savelli, B., Frey, N.F.D., 2019. Identification of new signalling peptides through a genome-wide survey of 250 fungal secretomes. *Bmc Genomics*. 20, 64.
- [27] Lin, X.H., Han, P., Dong, S.J., Li, H., 2015. Preparation and application of bacteriophage-loaded chitosan microspheres for controlling *Lactobacillus plantarum* contamination in bioethanol fermentation. *Rsc Adv*. 5(85), 69886-69893.
- [28] Liu, H., Hu, Z., Li, M., Yang, Y., Lu, S., Rao, X., 2023. Therapeutic potential of bacteriophage endolysins for infections caused by Gram-positive bacteria. *J. Biomed Sci*. 30(1), 29.
- [29] Liu, M., Bischoff, K.M., Gill, J.J., Mire-Criscione, M.D., Berry, J.D., Young, R., Summer, E.J., 2015. Bacteriophage application restores ethanol fermentation characteristics disrupted by *Lactobacillus fermentum*. *Biotechnol. Biofuels*. 8, 132.
- [30] Liu, X.M., Xu, W.J., Mao, L.Y., Zhang, C., Yan, P.F., Xu, Z.W., Zhang, Z.C., 2016. Lignocellulosic ethanol production by starch-based industrial yeast under PEG detoxification. *Sci. Rep*. 6, 20361.
- [31] Lu, S.Y., Bischoff, K.M., Rich, J.O., Liu, S., Skory, C.D., 2020. Recombinant bacteriophage LysKB317 endolysin mitigates *Lactobacillus* infection of corn mash fermentations. *Biotechnol. Biofuels*. 13, 157.
- [32] Lu, S.Y., Liu, S., Patel, M.H., Glezinski, K.M., Skory, C.D., 2023. *Saccharomyces cerevisiae* surface display of endolysin LysKB317 for control of bacterial contamination in corn ethanol fermentations. *Front. Bioeng. Biotechnol*. 11, 1162720.
- [33] Meneghin, S.P., Reis, F.C., de Almeida, P.G., Ceccato-Antonini, S.R., 2008. Chlorine dioxide against bacteria and yeasts from the alcoholic fermentation. *Braz. J. Microbiol*. 39(2), 337-343.
- [34] Monteiro, B., Ferraz, P., Baroca, M., da Cruz, S.H., Collins, T., Lucas, C., 2018. Conditions promoting effective very high gravity sugarcane juice fermentation. *Biotechnol. Biofuels*. 11.
- [35] Mumberg, D., Muller, R., Funk, M., 1995. Yeast vectors for the controlled expression of heterologous proteins in different genetic backgrounds. *Gene*. 156(1), 119-122.
- [36] Murray, E., Draper, L.A., Ross, R.P., Hill, C., 2021. The advantages and challenges of using endolysins in a clinical setting. *Viruses*. 13(4), 680.
- [37] Muthaiyan, A., Limayem, A., Ricke, S.C., 2011. Antimicrobial strategies for limiting bacterial contaminants in fuel bioethanol fermentations. *Prog. Energy Combust*. 37(3), 351-370.
- [38] Narendranath, N.V., Hynes, S.H., Thomas, K.C., Ingledew, W.M., 1997. Effects of lactobacilli on yeast-catalyzed ethanol fermentations. *Appl. Environ. Microbiol*. 63(11), 4158-4163.
- [39] Narendranath, N.V., Power, R., 2005. Relationship between pH and medium dissolved solids in terms of growth and metabolism of *Lactobacilli* and *Saccharomyces cerevisiae* during ethanol production. *Appl. Environ. Microbiol*. 71(5), 2239-2243.
- [40] Narendranath, N.V., Thomas, K.C., Ingledew, W.M., 2001. Effects of acetic acid and lactic acid on the growth of *Saccharomyces cerevisiae* in a minimal medium. *J. Ind. Microbiol. Biotechnol*. 26(3), 171-177.
- [41] Neubert, P., Halim, A., Zauser, M., Essig, A., Joshi, H.J., Zatorska, E., Larsen, I.S., Loibl, M., Castells-Ballester, J., Aebi, M., Clausen, H., Strahl, S., 2016. Mapping the *O*-Mannose Glycoproteome in *Saccharomyces cerevisiae*. *Mol. Cell. Proteomics*. 15(4), 1323-1337.
- [42] Paillet, T., Dugat-Bony, E., 2021. Bacteriophage ecology of fermented foods: anything new under the sun?. *Curr. Opin. Food. Sci*. 40, 102-111.
- [43] Patel, M.H., Lu, S.Y., Liu, S., Skory, C.D., 2023. Novel endolysin LysMP for control of *Limosilactobacillus fermentum* contamination in small-scale corn mash fermentation. *Biotechnol. Biofuels*. 16(1), 144.
- [44] Philippe, C., Cornuault, J.K., de Melo, A.G., Morin-Pelchat, R., Jolicoeur, A.P., Moineau, S., 2023. The never-ending battle between lactic acid bacteria and their phages. *Fems Microbiol. Rev*. 47(4).
- [45] Podlacha, M., Wegrzyn, G., Wegrzyn, A., 2024. Bacteriophages-Dangerous Viruses Acting Incognito or Underestimated Saviors in the Fight against Bacteria?. *Int. J. Mol. Sci*. 25(4), 2107.
- [46] Poljak, K., Selevsek, N., Ngwa, E., Grossmann, J., Losfeld, M.E., Aebi, M., 2018. Quantitative profiling of N-linked glycosylation machinery in yeast *Saccharomyces cerevisiae*. *Mol. Cell. Proteomics*. 17(1), 18-30.
- [47] Prins, R.C., Billerbeck, S., 2021. A buffered media system for yeast batch culture growth. *BMC Microbiol*. 21(1), 127.
- [48] Rahman, M.U., Wang, W., Sun, Q., Shah, J.A., Li, C., Sun, Y., Li, Y., Zhang, B., Chen, W., Wang, S., 2021. Endolysin, a promising solution against antimicrobial resistance. *Antibiotics*. 10(11), 1277.
- [49] Rich, J.O., Bischoff, K.M., Leathers, T.D., Anderson, A.M., Liu, S.Q., Skory, C.D., 2018. Resolving bacterial contamination of fuel ethanol fermentations with beneficial bacteria - an alternative to antibiotic treatment. *Bioresour. Technol*. 247, 357-362.
- [50] Rich, J.O., Leathers, T.D., Bischoff, K.M., Anderson, A.M., Nunnally, M.S., 2015. Biofilm formation and ethanol inhibition by bacterial contaminants of biofuel fermentation. *Bioresour. Technol*. 196, 347-354.
- [51] Roach, D.R., Khatibi, P.A., Bischoff, K.M., Hughes, S.R., Donovan, D.M., 2013. Bacteriophage-encoded lytic enzymes control growth of contaminating *Lactobacillus* found in fuel ethanol fermentations. *Biotechnol. Biofuels*. 6, 20.
- [52] Rossouw, M., Cripwell, R.A., Vermeulen, R.R., van Staden, A.D., van Zyl, W.H., Dicks, L.M.T., Viljoen-Bloom, M., 2023. Heterologous Expression of Plantaricin 423 and Mundtacin ST4SA in *Saccharomyces cerevisiae*. *Probiotics Antimicrob. Proteins*. 16, 845-861.
- [53] Rückle, L., Senn, T., 2006. Hop acids can efficiently replace antibiotics in ethanol production. *Int. Sugar J*. 108(1287), 139-147.
- [54] Salas-Navarrete, P.C., Rosas-Santiago, P., Suarez-Rodriguez, R., Martinez, A., Caspeta, L., 2023. Adaptive responses of yeast strains tolerant to acidic pH, acetate, and supraoptimal temperature. *Appl. Microbiol. Biotechnol*. 107(12), 4051-4068.
- [55] Schmelcher, M., Donovan, D.M., Loessner, M.J., 2012. Bacteriophage endolysins as novel antimicrobials. *Future Microbiol*. 7(10), 1147-1171.
- [56] Schwarz, C., Mathieu, J., Laverde Gomez, J.A., Yu, P., Alvarez, P.J.J., 2022a. Addition and correction to renaissance for phage-based bacterial control. *Environ. Sci. Technol*. 56(12), 9144.
- [57] Schwarz, C., Mathieu, J., Laverde Gomez, J.A., Yu, P., Alvarez, P.J.J., 2022b. Renaissance for phage-based bacterial control. *Environ. Sci. Technol*. 56(8), 4691-4701.
- [58] Seeboth, P.G., Heim, J., 1991. In-vitro processing of yeast alpha-factor leader fusion proteins using a soluble yscF (Kex2) variant. *Appl. Microbiol. Biotechnol*. 35(6), 771-776.
- [59] Silva, J.B., Sauvageau, D., 2014. Bacteriophages as antimicrobial agents against bacterial contaminants in yeast fermentation processes. *Biotechnol. Biofuels*. 7, 123.
- [60] Skinner-Nemec, K.A., Nichols, N.N., Leathers, T.D., 2007. Biofilm formation by bacterial contaminants of fuel ethanol production. *Biotechnol. Lett*. 29(3), 379-383.
- [61] Skinner, K.A., Leathers, T.D., 2004. Bacterial contaminants of fuel ethanol production. *J. Ind. Microbiol. Biotechnol*. 31(9), 401-408.
- [62] Szopinska, A., Christ, E., Planchon, S., Konig, H., Evers, D., Renaut, J., 2016. Stuck at work? Quantitative proteomics of environmental wine yeast strains reveals the natural mechanism of overcoming stuck fermentation. *Proteomics*. 16(4), 593-608.
- [63] Thomas, K.C., Hynes, S.H., Ingledew, W.M., 2002. Influence of medium buffering capacity on inhibition of growth by acetic and lactic acids. *Appl. Environ. Microbiol*. 68(4), 1616-1623.
- [64] Tian, J., Liang, Y.H., Ragauskas, A.J., Zhong, Y.M., Lin, Y.Q., 2024. Effects of AI-2 quorum sensing inhibitors on mitigating bacterial contamination in bioethanol production. *Biomass Bioenergy*. 184, 107211.
- [65] Tian, J., Lin, Y., Su, X., Tan, H., Gan, C., Ragauskas, A.J., 2023. Effects of *Saccharomyces cerevisiae* quorum sensing signal molecules on ethanol production in bioethanol fermentation process. *Microbiol. Res*. 271, 127367.

- [66] Topaloglu, A., Esen, Ö., Turanli-Yildiz, B., Arslan, M., Çakar, Z.P., 2023. From *Saccharomyces cerevisiae* to ethanol: unlocking the power of evolutionary engineering in metabolic engineering applications. *J. Fungi*. 9(10), 984.
- [67] Tse, T.J., Wiens, D.J., Reaney, M.J.T., 2021. Production of bioethanol—a review of factors affecting ethanol yield. *Fermentation*. 7(4), 268.
- [68] [Tyanova, S., Temu, T., Cox, J., 2016. The MaxQuant computational platform for mass spectrometry-based shotgun proteomics. *Nat. Protocol*. 11(12), 2301-2319.
- [69] U.S. Energy Information Administration, S.E.D.S.S., 2023. U.S. fuel ethanol production in the top five producing states and all others combined, 1981-2021, in: U.S. Energy Information Administration, S.E.D.S.S. (Ed.). State Energy Data System (SEDS).
- [70] van Eunen, K., Bouwman, J., Daran-Lapujade, P., Postmus, J., Canelas, A.B., Mensonides, F.I., Orij, R., Tuzun, I., van den Brink, J., Smits, G.J., van Gulik, W.M., Brul, S., Heijnen, J.J., de Winder, J.H., de Mattos, M.J., Kettner, C., Nielsen, J., Westerhoff, H.V., Bakker, B.M., 2010. Measuring enzyme activities under standardized *in vivo*-like conditions for systems biology. *FEBS J*. 277(3), 749-760.
- [71] Voth, W.P., Richards, J.D., Shaw, J.M., Stillman, D.J., 2001. Yeast vectors for integration at the *HO* locus. *Nucleic Acids Res.* 29(12), E59-59.
- [72] Walker, G.M., Basso, T.O., 2020. Mitigating stress in industrial yeasts. *Fungal Biol*. 124(5), 387-397.
- [73] Yamanishi, M., Ito, Y., Kintaka, R., Imamura, C., Katahira, S., Ikeuchi, A., Moriya, H., Matsuyama, T., 2013. A genome-wide activity assessment of terminator regions in *Saccharomyces cerevisiae* provides a "terminatome" toolbox. *ACS Synth. Biol*. 2(6), 337-347.



**Dr. Shao-Yeh Lu** is a Research Microbiologist at the U.S. Department of Agriculture, Agricultural Research Service, National Center for Agricultural Utilization Research in Peoria, Illinois, USA. Dr. Lu received his Ph.D. in Immunology and Infectious Diseases from Washington State University in 2018. He has authored numerous peer-reviewed journal articles on antimicrobial resistance and antimicrobial protein development.

His research interests include (1) the development of novel antimicrobial peptides, (2) the development of novel bacteriophage endolysin, and (3) bacterial contamination control in bioethanol fermentation in the Renewal Product Technology Research Unit. His research profile can be found at the following link:

<https://scholar.google.com/citations?hl=en&tzom=360&user=PhA1SEAAAAJ&authuser=1>



**Dr. Michael Bowman** is a Research Chemist at the USDA Agricultural Research Service, National Center for Agricultural Utilization Research in Peoria, Illinois, USA. He received his Ph.D. in Chemistry from Purdue University. As a member of the Bioenergy Research Unit, Dr. Bowman's research has focused on the use of analytical tools to identify enzymatic activities that improve the hydrolysis of biomass carbohydrate biopolymers.

That work advances the Bioenergy Research Unit's mission to develop bioproducts and bioprocesses for the conversion of agricultural commodities into biofuels and chemicals, enzymes, and polymers. The research profile for Dr. Bowman is available at:

<https://scholar.google.com/citations?user=qSHadZsAAAAJ&hl=en&oi=sra>



**Dr. Maulik Patel** is a Molecular Biologist and Bioinformatician specializing in genomic mining, functional genomics, and metabolic research. His work focuses on leveraging insights from genomic data and synthetic biology to enhance sustainability, particularly in green energy production, antimicrobials, and biomedical applications. An entrepreneur in the field of probiotics, Dr. Patel has developed a range of spore-based probiotics tailored for animal feed and biofertilizer use. He has also

contributed numerous articles exploring these innovations. In his free time, he enjoys reading, swimming, and delving into new, application-driven areas of research.



**Dr. Chris Skory** is a research microbiologist at the USDA Agricultural Research Service, National Center for Agricultural Utilization Research in Peoria, Illinois, USA. He obtained his PhD from Michigan State University and has subsequently published more than 100 research articles and numerous patents in fungal and yeast genetic engineering, novel antimicrobials, and fermentation biotechnology. Dr. Skory leads the Renewable Product Technology Research Group

to develop new and improved methods for the conversion of agricultural feedstocks, food waste, and processing byproducts to marketable value-added products, such as biofuels, biochemicals, bioplastics, alternative proteins, and/or functional food ingredients. His research profile is available at:

<https://scholar.google.com/citations?hl=en&authuser=1&user=OqIkNJoAAAAJ>



**Dr. Ronald Hector** is the Research Leader of the USDA Agricultural Research Service Bioenergy Research Unit at the National Center for Agricultural Utilization Research in Peoria, Illinois, USA. He received his B.S. in Chemical Engineering from Ohio University and Ph.D. in Molecular Genetics and Microbiology from the University of Florida. Ronald conducted postgraduate research on molecular mechanisms of DNA damage sensing and repair, as well as

telomere length regulation, at the Cleveland Clinic Lerner Research Institute. He has published over 60 peer-reviewed journal articles and 2 patents. His research currently focuses on developing microorganisms and fermentation processes for producing fuels and chemicals from agricultural materials. His research profile can be found at:

<https://www.scopus.com/authid/detail.uri?origin=AuthorProfile&authorId=56250693100&zone=> and

<https://scholar.google.com/citations?user=v2iKr54AAAAJ&hl=en&oi=sra>

Supplementary Material

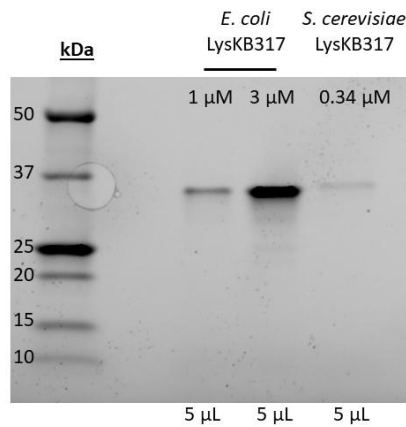


**Fig. S1.** SDS-PAGE (TGX stain-free gel) of purified recombinant LysKB317 from *E. coli* and *S. cerevisiae*. Purified recombinant endolysin from *E. coli* (intracellular) and *S. cerevisiae* (Y-2034 + KB; YPD spent media) were loaded in each well at 5  $\mu$ L. Calculated LysKB317 molecular weight is 33.8 kDa.

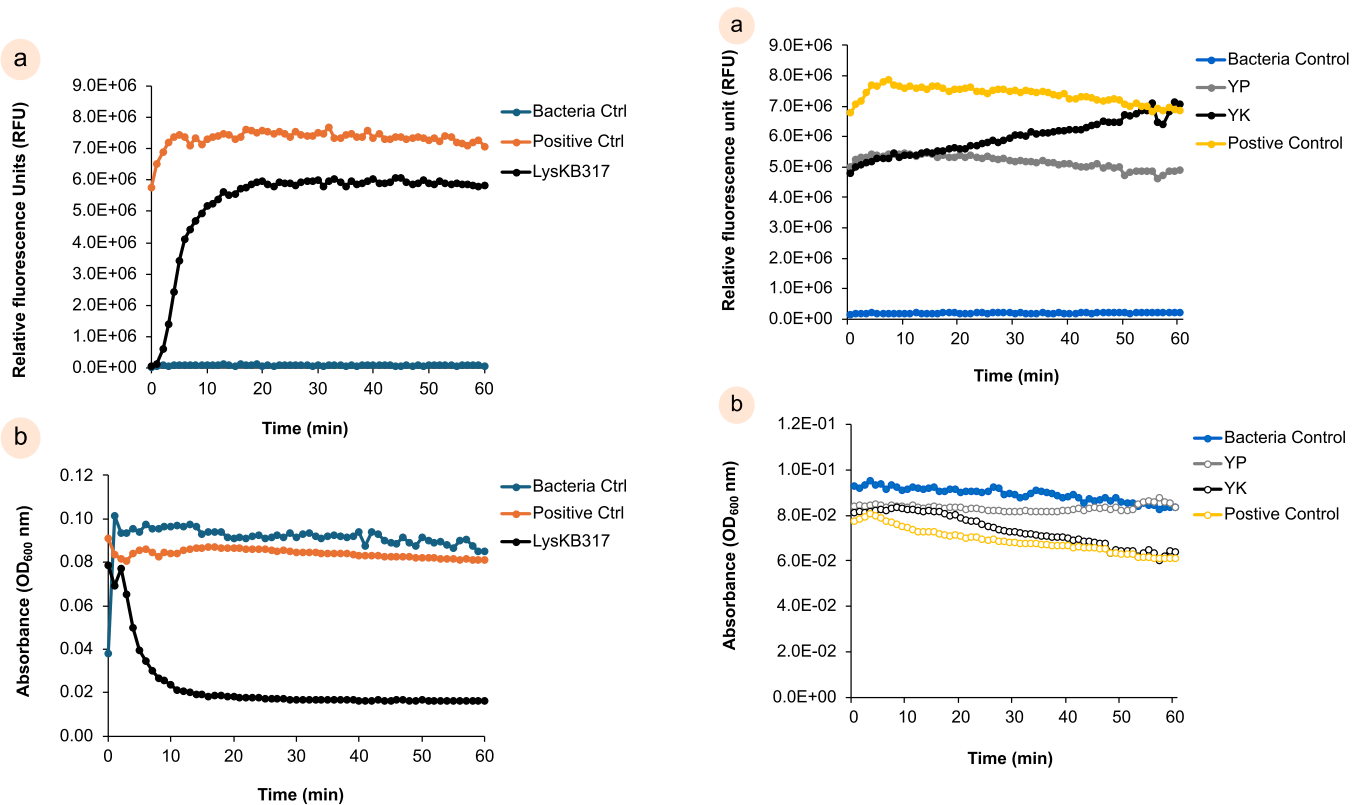


**Fig. S2.** Cell viability and turbidity assay controls of *E. coli* expressed LysKB317. (a) Relative fluorescence unit (RFU) measured of DNA staining by Sytox Green over time (60 min). Cell viability assay controls. *L. fermentum* cell wall degradation by isopropanol allowing staining of Sytox Green penetration to stain bacterial DNA (positive control; Orange); bacterial control without the addition of endolysin treatment showing limited staining (negative control (Blue)); Treatment of 1  $\mu$ M purified LysKB317 addition to *L. fermentum* showing bacterial cell wall lysis and DNA stain overtime (Black), and (b) Optical density measured at OD<sub>600</sub> nm overtime (60 min) with the same positive control (Orange), negative control (Blue) and treatment (Black).

**Fig. S3.** Cell viability and turbidity assay controls of *S. cerevisiae* expressed LysKB317. (a) Relative fluorescence unit (RFU) measured of DNA staining by Sytox Green over time (60 min). Cell viability assay controls. *L. fermentum* cell wall degradation by isopropanol allowing staining of Sytox Green penetration to stain bacterial DNA (positive control; Yellow); bacterial control without the addition of spent media containing endolysin treatment showing limited staining (negative control (Blue)); Treatment using spent media containing LysKB317 addition to *L. fermentum* showing bacterial cell wall lysis and DNA stain overtime (Y-2034 + KB; Black); Control treatment using spent media containing no LysKB317 from Y-2034 without LysKB317 integration (Gray), and (b) Optical density measured at OD<sub>600</sub>nm overtime (60 mins) with the same positive control (Yellow), negative control (Blue), treatment control (Black).

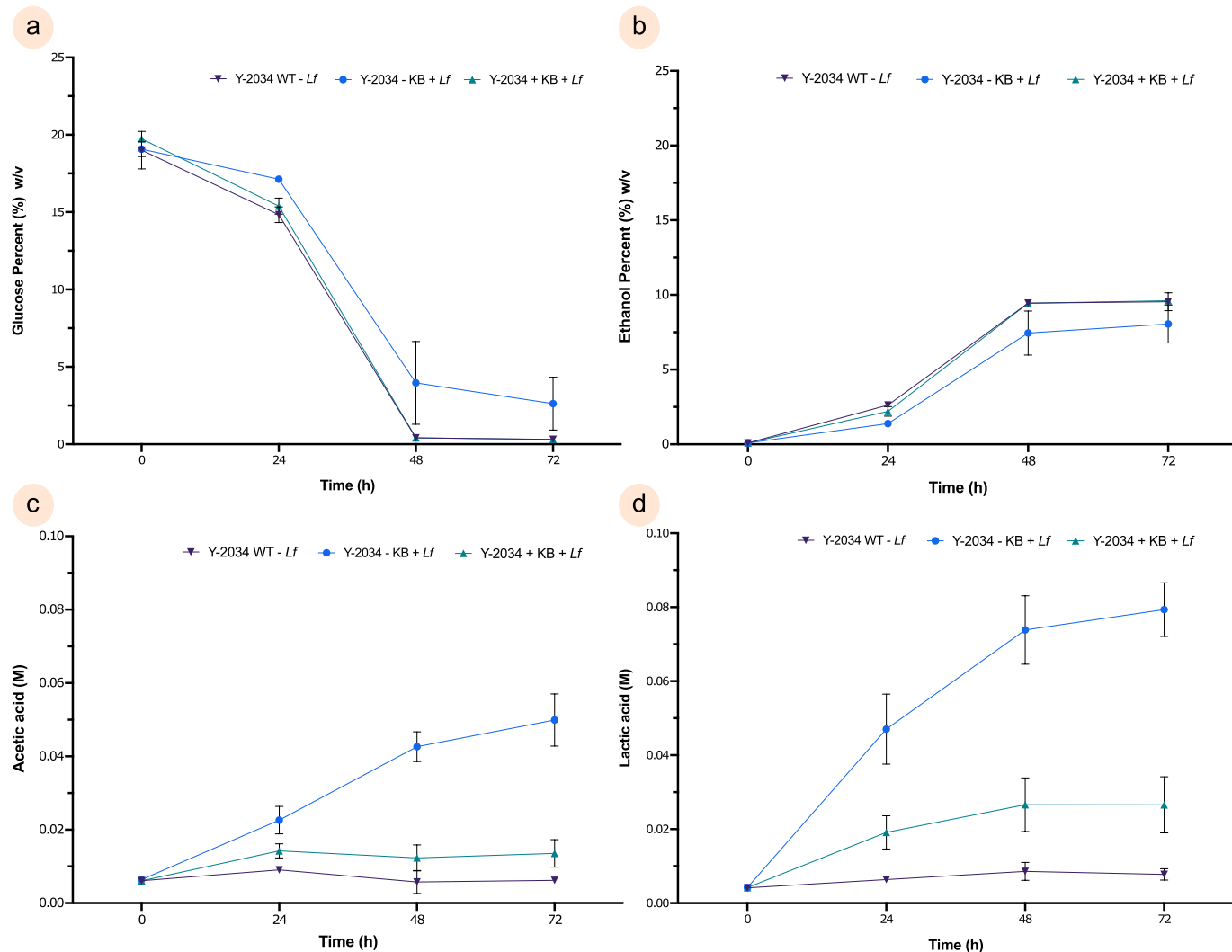


**Fig. S4. HPLC analysis of corn mash glucose and fermentation metabolites.** (a) Glucose consumption in percent (%) w/v; (b) Ethanol generated in percent (%) w/v; (c) molar (M) acetic acid; and (d) Molar (M) lactic acid. Yeast without LysKB317 gene integration (contamination control; Y-2034 - KB + Lf; Blue circle) and yeast with LysKB317 gene (Treatment; Y-2034 + KB + Lf; Triangle). The yeast-only control (Y-2034 WT; Inverted triangle) has no bacterial infection. All measurements were performed in three independent biological repeats ( $n = 3$ ) with mean  $\pm$  95% confidence intervals (CI) and statically determined based on two-way ANOVA.

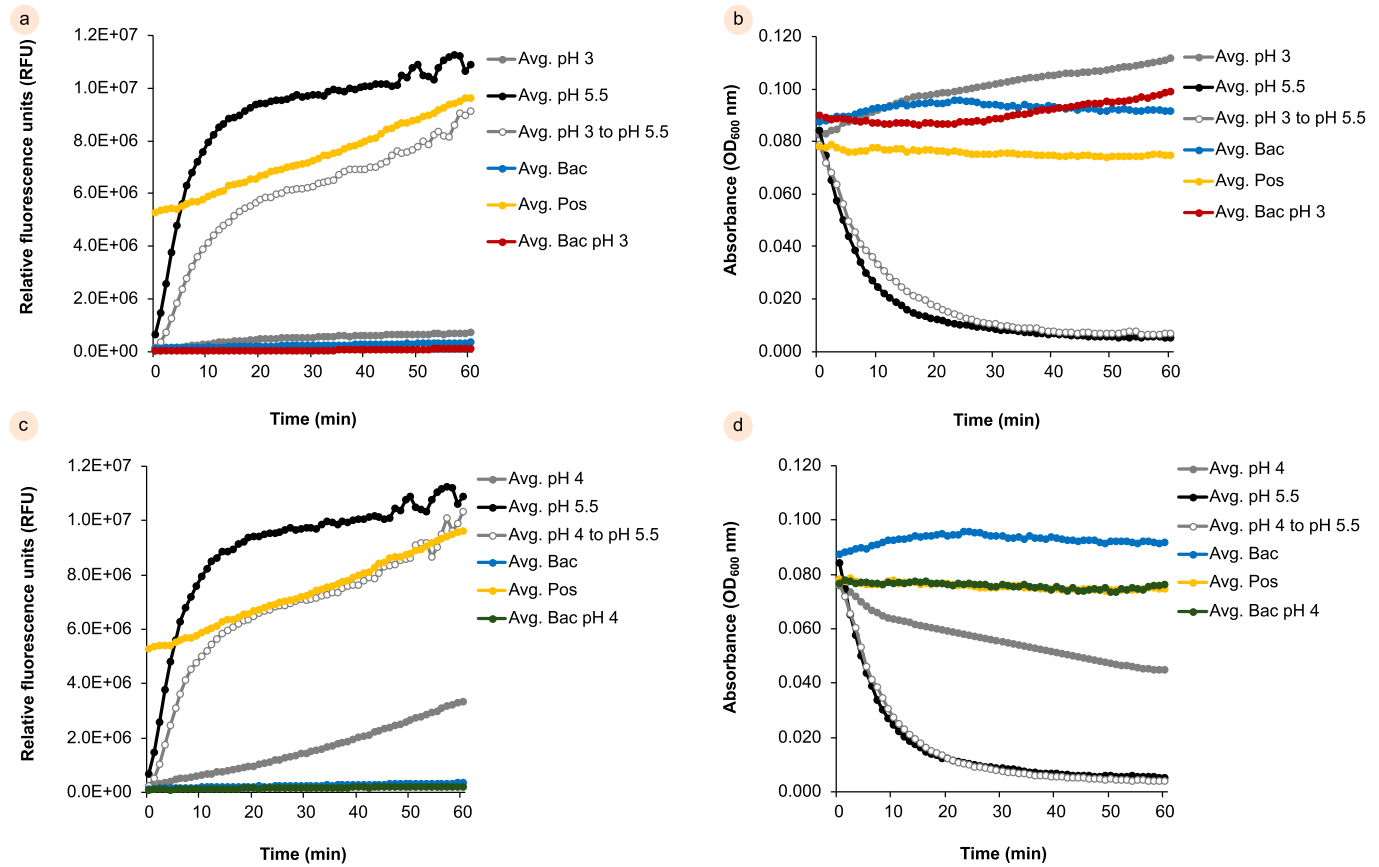
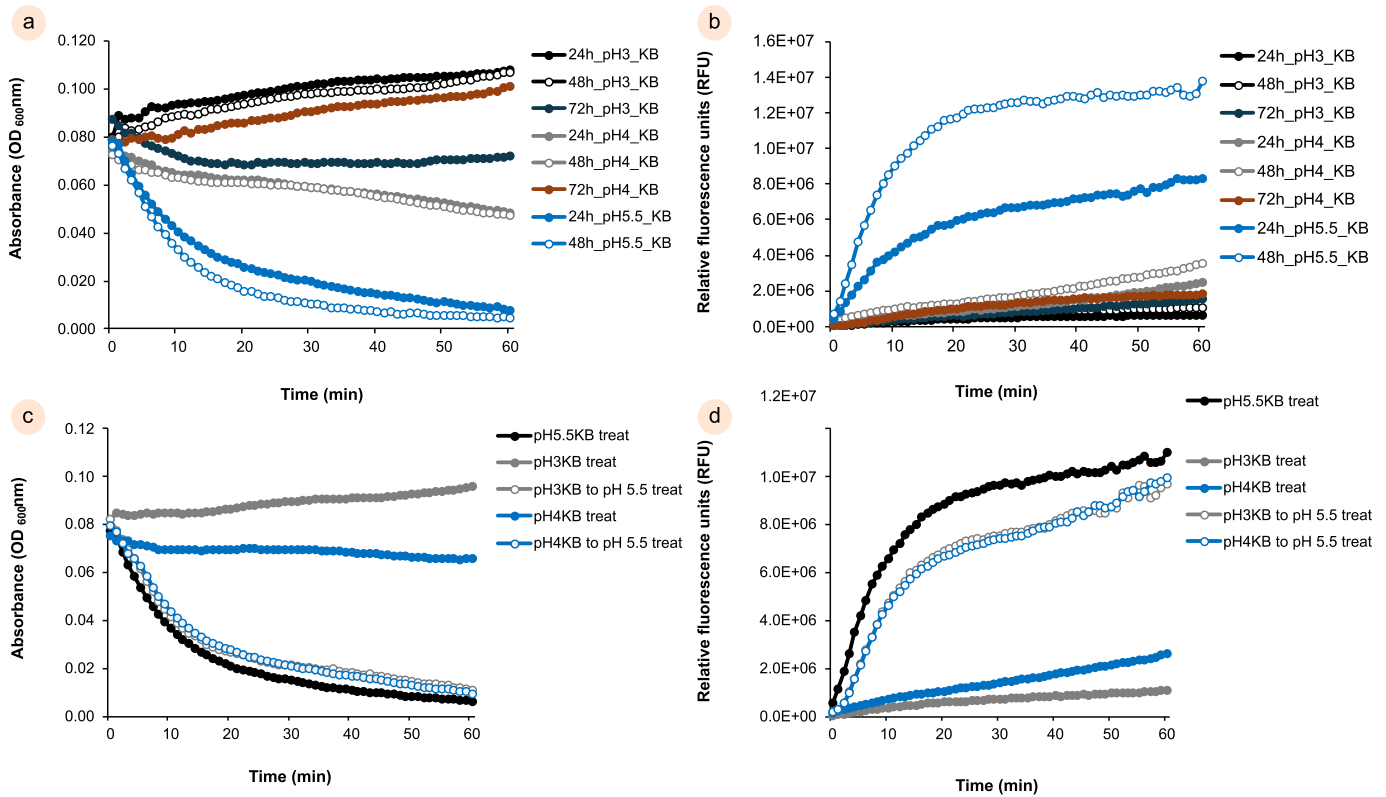
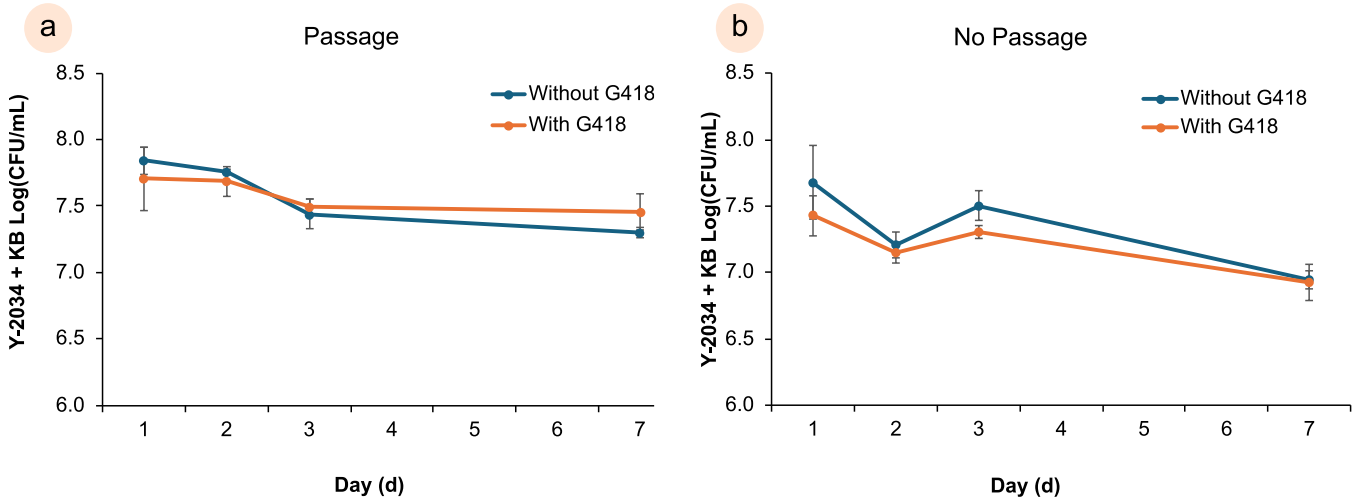


Fig. S5. Purified LysKB317 pH reversibility assay controls. (a) pH 3 to pH 5.5 enzyme reversibility detection using Sytox Green fluorescent dye; (b) Turbidity assay control for pH 3 to pH 5.5 LysKB317 reversibility measurement; (c) pH 4 to pH 5.5 enzyme reversibility detection using Sytox Green fluorescent dye; and (d) Turbidity assay control for pH 4 to pH 5.5 LysKB317 reversibility measurement.



**Fig. S6. Purified LysKB317 pH reversibility assay over 72 h.** (a) Turbidity assay measuring absorbance (OD<sub>600 nm</sub>) with purified LysKB317 (1  $\mu$ M) in pH 3, 4, and 5.5 buffer for 24 h, 48 h, and 72 h were measured over time (60 min) to determine exolytic activity against *L. fermentum* 0315-25; (b) Exolytic activity measured by relative fluorescence units (RFU) using a Sytox Green nucleic acid stain performed with purified LysKB317 (1  $\mu$ M) in pH 3, 4, and 5.5 buffer for 24, 48, and 72 h and assessed over time (60 min) to determine lytic activity against target bacteria; (c) The reversible activity of endolysin was examined when buffer pH was adjusted from pH 3 to pH 5.5 and pH 4 to pH 5.5 while comparing to pH 5.5 control condition. Turbidity assay showed recovery of activity (bacterial lysis) with re-adjusted buffer measured by a decrease in absorbance (OD<sub>600 nm</sub>); and (d) Samples of LysKB317 in pH re-adjusted buffer showed an increase in RFU signal indicating re-gaining lytic activity against *L. fermentum*.



**Fig. S7. Endolysin *HO*-locus integration stability.** A single colony of yeast (Y-2034 + KB) was taken and inoculated in 5 mL YPD at 30°C and 200 rpm with and without selection pressure (G418). Culture samples (100 µL) are taken daily (D1, D2, D3) for the first 3 days and at day 7 (D7). To determine the stability of the gene integration, we use an Eddy Jet 2 spiral plater (IUL Instruments) set in the E mode 50 (50 µL sample). Samples are diluted in the ratio of 1:1,000 using ultrapure sterile water. Plated samples were incubated at 30°C overnight, and yeast colonies were enumerated using a Flash & Go plate reader (IUL Instruments) with a minimum of detection limits predetermined at > 3-log (CFU/mL) per sample. Each condition was performed in 3 biological replicates ( $n = 3$ ) and standard deviation (SD) as the error bar. (a) Daily passage (1:100 ratio) into fresh 5 mL YPD tubes containing selective pressure G418 (orange) and without G418 (dark teal) showed no significant difference between the conditions, and (b) Continuous growth for 7 days without passage, with and without G418 selection pressure showed no significant difference. Both figures suggest stable integration of the LysKB317 gene into the *HO*-locus.

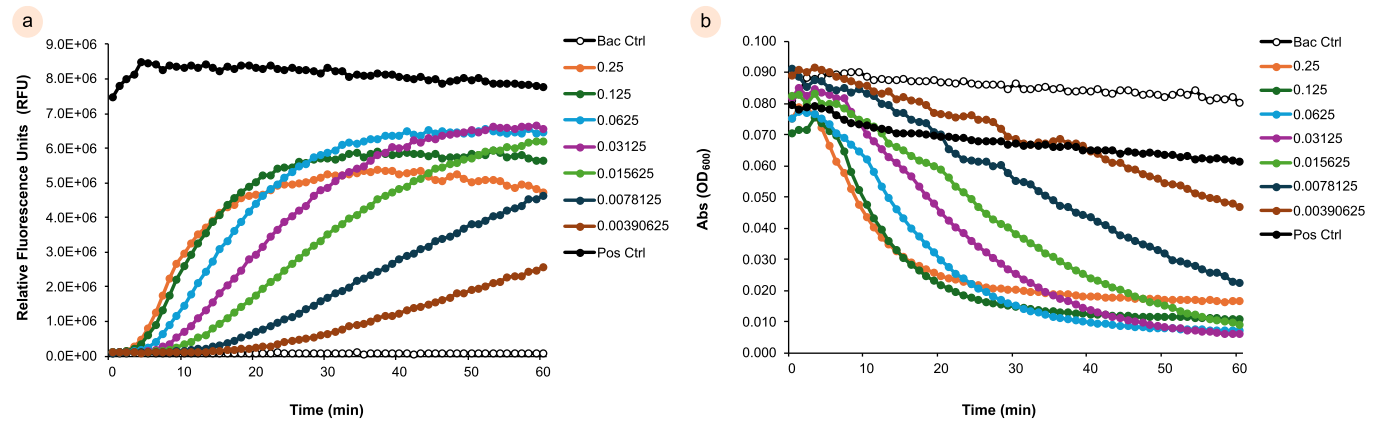


**Fig. S8. Bacterial viability assay and turbidity assay on LysKb317 concentration gradient sensitivity.** (a) Cell viability conducted with exogenous addition of LysKB317 at 0.0039 – 0.25 µM against *L. fermentum* with SYTOX Green nucleic acid stain to examine exolytic activity for 1 h, and (b) Turbidity assay against *L. fermentum* measured at optical density 600 nm (OD<sub>600</sub> nm) for 1 h.